2018-10-23

Sustainable Concrete Using Seawater and Glass Fiber Reinforced Polymer Bars

Morteza Khatibmasjedi
University of Miami, mortezakhatib@gmail.com

UNIVERSITY OF MIAMI

SUSTAINABLE CONCRETE USING SEAWATER AND GLASS FIBER REINFORCED POLYMER BARS

By

Morteza Khatibmasjedi

A DISSERTATION

Submitted to the Faculty
of the University of Miami
in partial fulfillment of the requirements for
the degree of Doctor of Philosophy

Coral Gables, Florida

December 2018

UNIVERSITY OF MIAMI

A dissertation submitted in partial fulfillment of
the requirements for the degree of
Doctor of Philosophy

SUSTAINABLE CONCRETE USING SEAWATER AND GLASS FIBER REINFORCED POLYMER BARS

Morteza Khatibmasjedi

Approved:

_____
Antonio Nanni, Ph.D.
Professor and Chair of Civil, Architectural, and Environmental Engineering

_____
Prannoy Suraneni, Ph.D.
Assistant Professor of Civil, Architectural, and Environmental Engineering

_____
Ali Ghahremaninezhad, Ph.D.
Assistant Professor of Civil, Architectural, and Environmental Engineering

_____
Guillermo Prado, Ph.D.
Dean of the Graduate School

_____
Tyler Ley, Ph.D.
Professor of School of Civil and Environmental Engineering
Oklahoma State University

KHATIBMASJEDI, MORTEZA (Ph.D., Civil Engineering)

Sustainable Concrete using Seawater and Glass Fiber Reinforced Polymer Bar

(December 2018)

Abstract of a dissertation at the University of Miami.

Dissertation supervised by Professor Antonio Nanni.
No. of pages in text. (90)

In order to improve the sustainability of the construction industry, which is responsible for 12 % of all fresh-water consumption, seawater could be an advantageous replacement for fresh water in mixing concrete especially in coastal regions where fresh water may be scarce. Seawater could potentially be used in unreinforced concrete and mortar (i.e. bricklaying, renders, etc.) or in combination with non-corrosive reinforcement (i.e. Glass Fiber Reinforced Polymer (GFRP) bars). In order to achieve the widespread usage of such technology, the fundamental behavior of seawater-mixed concrete and embedded GFRP bars need to be studied. This dissertation consists of three studies which cover the durability of GFRP bars in seawater-mixed concrete (*Study 1*), compressive strength of seawater-mixed concrete under different curing regimes (*Study 2*), and shrinkage behavior of seawater-mixed concrete (*Study 3*).

Study 1 investigates the effect of seawater used as mixing water in concrete on the long-term properties of GFRP bars. The durability of GFRP bars embedded in seawater-mixed concrete was studied in terms of residual mechanical properties (i.e. tensile strength, horizontal and transverse shear strength, and GFRP-concrete bond strength) after immersion in seawater at 60 °C for a period of 24 months. Benchmark specimens were also

cast using conventional concrete. Results showed comparable performance between the two sets of bars. Some degradation of the mechanical properties was observed in both cases, with the most degradation being observed in the bond strength. Tensile strength decreased by 21 – 26%, tensile modulus by 6 – 12%, horizontal shear strength by 21 – 26%, and transverse shear strength by 25 – 28%. The bond strength showed the highest degradation, with 47 and 55% reductions for bars extracted from conventional and seawater-mixed concrete, respectively. Scanning electron microscopy was used to identify degradation mechanisms. Areas with large concentrations of voids near the bar edge, formed during manufacturing, may provide a pathway for moisture and alkalis into the bar which could lead to fiber disintegration and debonding between fibers and the resin. Over time, a greater number of fibers are affected, which leads to the formation of significant cracking near the edge. This could explain the greater degradation in bond strength.

Study 2 reports the results of an investigation on the effect of different environments (curing regimes) on the compressive strength development of seawater-mixed concrete. Fresh properties of concretes prepared with seawater and concrete mixed with tap water were comparable, except for set times, which were accelerated in seawater-mixed concretes. Concrete cylinders were cast and exposed to subtropical environment (outdoor exposure), tidal zone (wet-dry cycles), moist curing (in a fog room), and seawater at 60 °C (140 °F) (submerged in a tank). Under these conditions, seawater-mixed concrete showed similar or better performance when compared to conventional concrete. In order to further understand strength development of such mixtures, Thermogravimetric Analysis (TGA), Energy-dispersive X-ray spectroscopy (EDX), and electrical resistivity measurements were performed at the end of 24 months on specimens exposed to seawater at 60 °C (140

°F). In this curing regime, concrete mixed with seawater constantly performed better than conventional concrete by 10 – 18% over the 24 months. The reason for the better performance is lower leaching of the calcium hydroxide from the concrete mixed with seawater, due to a reduction in ionic gradients between the pore solution and curing solution in concrete mixed with seawater. These results suggest that concrete mixed with seawater can potentially show better performance when compared to conventional concrete for marine and submerged applications due to lower leaching.

The shrinkage behavior of cementitious materials mixed with seawater is investigated in *Study 3*. Cement mortar mixtures were prepared with two water-to-cementitious materials ratios (w/cm = 0.36 and 0.45), two binder compositions (namely, ordinary Portland cement (OPC) and OPC with 20 % fly ash replacement), and two types of water (tap water and seawater). The autogenous and drying shrinkage behavior of these mixtures are examined using ASTM standard test methods for 65 days. The use of seawater as mixing water increased the autogenous shrinkage. At w/cm 0.36, the ultimate autogenous shrinkage increased from 213 μs in the mixture with tap water to 387 μs in the mixture with seawater; corresponding values were 149 μs and 314 μs for mixtures with w/cm 0.45. An acceleration of the cement hydration at early ages due to the seawater is identified as the cause of the increase in autogenous shrinkage in mixtures with seawater. At w/cm 0.36, seawater did not have a strong effect on the drying shrinkage and tested mixtures had ultimate drying shrinkage values between 543 μs and 663 μs. At w/cm 0.45, in mixtures without fly ash, ultimate drying shrinkage increased from 838 μs in the mixture with tap water to 1027 μs in the mixture with seawater. In mixtures with fly ash, the ultimate drying shrinkage increased from 738 μs in the mixture with tap water to 1370 μs in the mixture

with seawater. The drastic increase in the drying shrinkage in mixtures containing fly ash and seawater at w/cm 0.45 seems to be due to the development of a finer pore size distribution and internal water movement. In applications where drying shrinkage may be a concern, the use of fly ash in seawater-mixed concrete could be problematic.

To my parents, my sister, my uncle Dr. Reza Khatib, and my beautiful wife Haley.

ACKNOWLEDGEMENTS

I would like to express my sincerest gratitude and appreciation to my advisors Dr. Antonio Nanni and Dr. Tyler Ley for their guidance and support during my graduate studies. I am extremely grateful and thankful to Dr. Prannoy Suraneni. Without his mentorship, knowledge, and guidance, this would not have been possible. Thank you to my friend and colleague, Siva, for your help and support. I would like to express my gratitude to INFRAVATION program and ACI Foundation's Concrete Research Council for the support provided.

TABLE OF CONTENTS

LIST OF FIGURES

LIST OF TABLES

CHAPTER 1

INTRODUCTION

The World Health Organization estimates insufficiency of drinking water for over half of the population of the world by 2025 [1]. In addition, natural disasters frequently lead to fresh water shortages in affected regions. The building industry is responsible for about 12% of all fresh-water use [2]. Most of this fresh water is used to wash aggregates, mix concrete, and to cure concrete. As the population of the world is increasing rapidly, there is a high demand for concrete, as it is the most widely used construction material. In order to conserve fresh water, a finite resource, it is imperative that the construction industry looks for alternatives for fresh water usage. Seawater, which constitutes 96.5 % of the water available on earth [3], could be a potentially advantageous replacement for fresh water in mixing concrete especially in coastal regions where fresh water may be scarce. Using seawater as mixing water in concrete leads to an increase in concrete sustainability as seawater is a renewable resource, compared to potable water which is mostly a non-renewable resource [4]. Seawater could potentially be used in unreinforced concrete and mortar (i.e. bricklaying, renders, etc.) which comprise 55 % of the construction materials made with cement [5]. There are several unreinforced concrete structures along the coasts of Los Angeles and Florida which have used seawater for mixing and curing concrete and have shown no significant long-term degradation at the time of inspection [6, 7]. The use of seawater in reinforced concrete (RC) is generally prohibited due to fears regarding chloride-induced corrosion of steel reinforcement [8]. However, non-corrosive reinforcement such as Glass Fiber Reinforced Polymer (GFRP) could potentially be used

to reinforce the seawater-mixed concrete. GFRP has shown promise as a replacement for steel in chloride-rich environments, such as marine structures, due to its non-corrosive nature [9].

Glass fiber reinforced polymer (GFRP) bars are fabricated of continuous fibers impregnated in a polymeric resin matrix via the pultrusion process. The load is carried by the fiber and transferred by the resin. The resin also protects and binds the fibers together. Glass is the most commonly used fiber with many advantageous characteristics. GFRP is of high strength and high chemical resistance and it is relatively of low cost when compared to other fiber reinforced polymers such as carbon FRP. Matrices are typically thermosetting resins with vinyl ester because of its adequate mechanical characteristics and superb resistance to corrosion. The weight of FRP bars are about one-fourth that of conventional steel. This is particularly useful for reducing the cost of transportation and for also making it easier for handling the bars at the job site. The tensile stress-strain relationship of GFRP bars is linear elastic up to failure. GFRP bars possess higher tensile strength but lower modulus of elasticity and ultimate tensile strain when compared to steel bars. The mechanical properties of a GFRP bar are affected by environmental conditions. The tensile/bond characteristics of GFRP, may be affected by moisture, acidic or alkaline solutions, extreme temperature or ultraviolet exposure [16]. However, research has shown that by improving the manufacturing technique over time, the quality and durability of the bars has also improved.

Before widespread implementation of such technology may be achieved, it is important to understand the fundamental behavior of concrete mixed with seawater and embedded

GFRP bars. To this end, this dissertation focuses on three main areas presented as following:

Study 1: Durability of GFRP Reinforcement in Seawater-Mixed Concrete under Accelerated Aging Conditions

Study 2: Compressive Strength Development of Concrete Mixed with Seawater Subject to Different Curing Regimes

Study 3: Shrinkage Behavior of Cementitious Materials Mixed with Seawater

Study 1 aims to assess the long-term durability of GFRP bars in seawater-mixed concrete using accelerated aging. This study evaluates the durability of GFRP bars embedded in seawater-mixed concrete and conventional concrete and immersed in seawater at 60 °C for 24 months. Residual mechanical properties (i.e., tensile properties, horizontal and transverse shear strengths, and bond strength) of the GFRP bars, and the reasons behind their degradation are discussed. This work, entitled, "Durability of GFRP Reinforcement in Seawater-Mixed Concrete under Accelerated Aging Conditions", has been submitted to Journal of Composites for Construction for consideration for publication.

Study 2 compares the performance of conventional concrete and seawater-mixed concrete in various environments. Concrete cylinders were cast and exposed to subtropical environment (outdoor exposure), tidal zone (wet-dry cycles), moist curing (in a fog room), and seawater at 60 °C (140 °F) (submerged in a tank). In addition, a set of specimens exposed to one curing condition (immersion in seawater at 60 °C [140 °F]) are studied using thermogravimetric analysis (TGA), energy-dispersive X-ray spectroscopy (EDX), electrical resistivity, water absorption, and density measurements in order to explain the better performance of seawater-mixed concrete under certain curing regimes. This work,

entitled, “Compressive Strength Development of Concrete Mixed with Seawater Subject to Different Curing Regimes”, has been submitted to ACI Materials Journal for consideration for publication.

Study 3 investigates the drying and autogenous shrinkage behavior of cementitious materials mixed with seawater. Cement mortar mixtures with two water-to-cementitious materials ratios (w/cm = 0.36 and 0.45), two binder compositions (namely, ordinary Portland cement [OPC] and OPC with 20 % fly ash replacement), and mixed with two types of water (tap water and seawater) were examined. Differences in shrinkage behavior are correlated to changes in mass, hydration, pore solution composition, porosity, and pore size distribution. This work, entitled, “Shrinkage Behavior of Cementitious Materials Mixed with Seawater”, is currently in preparation for submission to Advances in Civil Engineering Materials.

Research Significance

In order to achieve the widespread usage of seawater-mixed concrete, the fundamental behavior of concrete mixed with seawater and embedded GFRP bars must be understood. Despite the vast amount of research on GFRP bar durability [10-16], the long-term properties of the bond between GFRP and concrete have not been studied in detail [13, 15]. To the best knowledge of the author, this has never been studied with seawater-mixed concrete. It is also unclear whether the high concentrations of certain ions (i.e., chloride, sodium, potassium, etc.) in the seawater might result in a reduced durability of the GFRP reinforcement. The results presented in *Study 1* help to fill this research gap.

While several studies have looked at the long-term performance of concrete mixed with seawater, little research has been performed on a direct comparison of conventional concrete and seawater-mixed concrete in various environments, and this is the objective of *Study 2*. This study shows why different later-age strength development in conventional concrete and seawater-mixed concrete may be expected and identifies environmental regimes in which it may be advantageous to use concrete mixed with seawater.

Shrinkage can cause concrete cracking, which increases the ingress of deleterious species into the concrete, which can lead to a reduction in the service life. To the best knowledge of the author, very little research has been performed on the shrinkage behavior of seawater-mixed concrete. *Study 3* covers this research gap by investigating the autogenous and drying shrinkage behavior of seawater-mixed cement mortar mixtures.

CHAPTER 2

STUDY 1: DURABILITY OF GFRP REINFORCEMENT IN SEAWATER-MIXED CONCRETE UNDER ACCELERATED AGING CONDITIONS

Background

The current study aims to assess the long-term durability of GFRP bars in seawater-mixed concrete using accelerated aging, as there are no existing seawater-mixed concrete structures reinforced with GFRP bars. Long-term performance of GFRP reinforcement in conventional concrete has been studied using field and accelerated aging data [9, 17]. Concrete cores with GFRP bars from a bridge in service for 15 years have been extracted and no significant changes in GFRP microstructural properties, chemical composition, glass transition temperature (T_g), and fiber content were observed [18]. A study on GFRP bars in five to eight year old concrete structures exposed to natural environments did not show any changes in the resin matrix and T_g of extracted GFRP bars compared to GFRP bars preserved under controlled laboratory conditions [19]. Based on these results, it was concluded that GFRP bars were "intact" after being in service for that specific period of time.

Several studies have employed elevated temperature as the acceleration factor in order to examine durability of GFRP reinforcement in concrete structures [13, 17, 20-24]. Degradation of GFRP bars mainly depends on the alkali diffusion and silica dissolution rates in alkaline environment, both of which are accelerated by elevated temperatures [25, 26]. The Arrhenius model has been used to correlate data from accelerated aging to long-term durability of GFRP bars [27]. Most studies addressed aged bars in simulated concrete

pore solutions [17, 20-22], but only few studies were performed on GFRP bars embedded in concrete, which better represents field conditions [13, 23, 24]. Even fewer studies have been performed on GFRP bars embedded in concrete and exposed to saline solutions, which represents marine conditions [23, 24].

A study of mortar-wrapped GFRP bars immersed in 3% NaCl solutions at 23, 40, 50, and 70 °C for 365 days did not show significant degradation in tensile properties and microstructure, even at high temperatures [23]. The residual strength of two types of GFRP bars embedded in seawater-mixed concrete immersed in tap water at 20, 40, and 60 °C for 450 days has been studied [24]. The authors found different performance for two types of GFRP bars – tensile strength reduction was 2 – 15% for the GFRP bar Type I and 19 – 50% for GFRP bar Type II [24]. In agreement with other literature [9, 28], the authors concluded that durability of GFRP reinforcement is highly dependent on the bar void content and moisture absorption, which are affected by chemical composition of the resin, characteristics of the fiber-resin interface, and interfacial imperfections that may develop during the manufacturing process.

Despite the vast amount of research on GFRP bar durability [10-16], the long-term properties of the bond between GFRP and concrete have not been studied in detail [13, 15]. To the author's best knowledge, this has never been studied with seawater-mixed concrete. It is unclear whether the high concentrations of certain ions (i.e., chloride, sodium, potassium, etc.) in the seawater might result in a reduced durability of the GFRP reinforcement.

The current study evaluates the durability of GFRP bars embedded in seawater-mixed concrete and conventional concrete and immersed in seawater at 60 °C for 24 months.

Residual mechanical properties (i.e., tensile properties, horizontal and transverse shear strengths, and bond strength) of the GFRP bars, and the reasons behind their degradation are discussed.

Experimental Materials and Methods

Characterization of Raw Materials

Concrete – A type II cement meeting the requirements of ASTM C150 [29] and a type F fly ash conforming to ASTM C618-17a [30] were used in this study. Tap water and seawater from Key Biscayne Bay (FL) were used as mixing water, respectively, with chemical composition (determined by inductively coupled plasma) as shown in **Table 1**. Further details are presented elsewhere [31]. Miami oolite with a nominal maximum aggregate size of 25 mm was used as the coarse aggregate and silica sand as the fine aggregate.

Table 1 Chemical composition of tap water and seawater used in concrete mixtures.

Ions	**Concentration (ppm)**	
	Tap Water	**Seawater**
Calcium	90	389
Chloride	44	18759
Iron	-	0.512
Potassium	6	329
Magnesium	6	1323
Sodium	26	9585

Sulfate	8	2489
Nitrate	1	0.134

GFRP – The bars were made of boron-free E-CR glass fibers embedded in a vinyl ester resin. The bar manufacturer did not disclose the presence and amounts of fillers and additives to the resin system other than stating that the GFRP bars are in compliance with AC 454 [32]. The bars had a double helically twisted wrapped fiber as a surface enhancement. The mechanical and physical properties of 15.8 mm diameter unaged GFRP bars, serving as the benchmark, were examined per ASTM standards and summarized in **Table 2**. Further details on the testing of GFRP bars are presented elsewhere [9]. Five repetitions were performed for each test and the coefficient of variation (CoV, %) for the collected data is also provided in **Table 2**. A close-up picture of the GFRP bar used in this study is shown in **Fig. 1**.

Table 2 Physical and mechanical properties of the pristine bars.

Material Property		**ASTM Standard**	**Unit**	**Value**	**CoV%**
Physical	Cross-sectional area	D792	mm^2	220.9	0.66
	Fiber content	D2584	% vol.	76.2	0.82
	Moisture absorption	D570	%	0.23	5.90
Mechanical	Tensile strength	D7205	MPa	1132.0	2.20
	Tensile chord modulus	D7205	GPa	52.7	3.50
	Horizontal shear strength	D4475	MPa	35.5	3.00

	Transverse shear strength	D7617	MPa	181.0	5.20

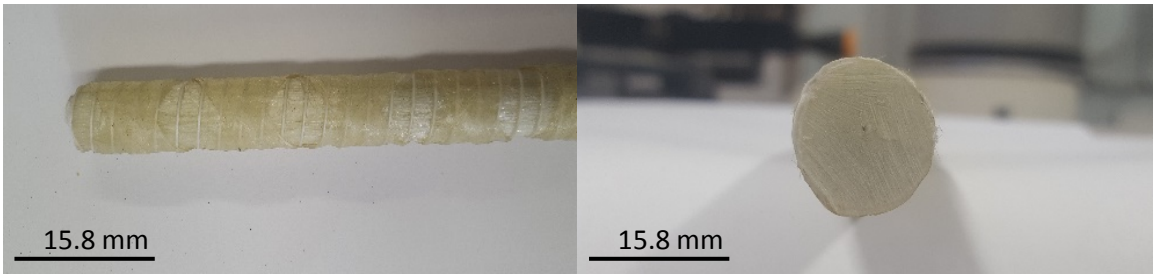

Fig. 1 Close-up picture of the GFRP bar.

Concrete Mixtures

Reinforced concrete specimens from two different mixtures with the water to cementitious materials ratio of 0.40 were cast: Mix A is the reference conventional concrete, and Mix B is the seawater-mixed concrete. The mixture proportions of Mix B are identical to those of Mix A, but fresh water is substituted with seawater from Key Biscayne Bay (Florida). **Table 3** shows the mixture proportions. Further details about the concrete are presented elsewhere [39].

Table 3 Mixture proportions.

Material	**Units**	**Mix A**	**Mix B**
Portland cement I-II (MH)	kg/m^3	332	332
Fly ash	kg/m^3	83	83
Tap water	kg/m^3	168	-
Seawater	kg/m^3	-	168
Coarse aggregate	kg/m^3	1038	1038
Fine aggregate	kg/m^3	612	612

Set retarding admixture	ml/m^3	-	830
Air-entraining admixture	ml/m^3	310	310

Durability of GFRP Bars in Seawater Concrete

Accelerated Aging – For all tests except the bond strength test, GFRP bars were embedded in concrete elements (beams) made from the two mixtures with dimensions of 152 x 190 x 1,422 mm with a minimum 30 mm concrete cover. Each specimen was reinforced with four GFRP bars, 1,360 mm long, and immersed in seawater at 60 °C as accelerated conditioning. The configuration of the reinforced specimens is shown in **Fig. 2**. This environment increases the diffusion rate of the concrete pore solution into the GFRP bars and accelerates chemical degradation processes for the same time of immersion [26]. Aside from self-weight, no load was applied to the beams during conditioning. Every six months, elements were removed from the hot seawater chamber and the bars were extracted from the concrete by splitting the concrete beams using a hammer drill. Extreme caution was exercised in the extraction so as not to damage the bars. Extracted bars were tested in terms of residual tensile properties and horizontal and transverse shear strength as indicators of degradation due to exposure. ASTM test methods were used with at least three repetitions per test. Tests were performed at room temperature 48 hours after the extraction. This time period is needed to install the steel-pipe anchors for tensile tests; all specimens were dried at room temperature for 48 hours before mechanical tests.

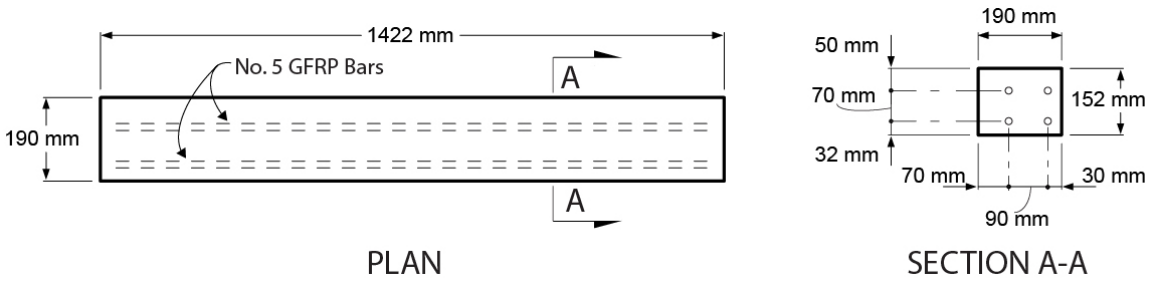

Fig. 2 Configuration of the reinforced specimens.

Tensile Properties – The ultimate tensile strength and tensile chord modulus of elasticity of extracted GFRP bars after 6, 12, 18, and 24 months exposure to the combination of concrete environment and accelerated conditioning were examined per ASTM D7205/D7205M-06(2016) [36]. Steel-pipe anchors were used and each specimen was instrumented with a linear variable differential transformer (LVDT) to capture elongation during testing.

Horizontal Shear Strength – The horizontal shear strength of the extracted GFRP bars was determined per ASTM D4475-02(2016) [37]. GFRP segments, 82 mm long (span-to-diameter ratio five) were center-loaded. The ends of the specimen rested on two supports that allowed the specimen to bend. The load was applied at a rate (of crosshead motion) of 1.3 mm/min. The specimen was deflected until shear failure occurred at the mid-plane of the horizontally-supported bar.

Transverse Shear Strength – Extracted GFRP bars were cut into 228-mm long segments and fitted into a double-shear fixture with appropriate cutting blades and clamped into place as per ASTM D7617/D7617M-11(2017) [38]. The shear fixture was then mounted into a universal mechanical testing machine and loaded to failure while recording force and crosshead displacement.

Bond Strength of GFRP Bars – The specimens used for the bond strength were as per ASTM D7913/D7913M-14 [40]. For this test, 200-mm seawater-mixed and conventional concrete cubes with the mixture design as in **Table 3** and embedded 10-mm diameter GFRP bar (of the same type of bars as the ones detailed in **Table 2** and **Fig. 1**) were cast and exposed to seawater at 60 °C. The total bond length was 5d, where d is the bar diameter. Every six months, at least three cubes from each mixture were removed from the hot seawater chamber and the bond strength between the GFRP bar and concrete was determined by pull out testing per ASTM D7913/D7913M-14 [40]. The steel-pipe anchor was used at the loading-end and an LVDT was used at the free-end of GFRP bars to measure slip. The bearing surface of the concrete cube was placed in contact with the loading plate. Tensile loading at the rate of 20 kN /min was applied and continued until the force decreased and the free-end slip was at least 2.5 mm.

Microstructural Studies – Extracted GFRP specimens were polished using different grit levels (i.e., 180, 300, 600 and 1200) of sand paper using grinding and polishing equipment. The specimens were then fine polished using a wet-polishing agent and 3 and 1 μm polycrystalline diamond paste. Prior to imaging, specimens were placed in an oven at 50 °C for 24 h to remove any moisture introduced during embedment in concrete and polishing. Samples were then cleaned using an ultrasonic cleaner and gold-coated prior to imaging. Scanning Electron Microscopy (SEM) imaging and Energy-Dispersive X-ray (EDX) spectroscopy were utilized to inspect the microstructure and chemical composition of the extracted bars in order to better explain degradation mechanisms, both physical and chemical. Both backscatter and secondary imaging were used. While the exact setting

parameters varied, typical settings are: Voltage = 15 kV, Working Distance = 12 mm, Spot Size = 60, Magnification = 500x, and Dead Time = 19 – 23%.

Results and Discussion

Tensile Properties

All specimens failed by rupture. The results for the tensile strength and tensile chord modulus of elasticity of the extracted GFRP bars after 6, 12, 18, and 24 months exposure to the combination of concrete environment and accelerated conditioning are presented in **Fig. 3** and **Fig. 4**, respectively.

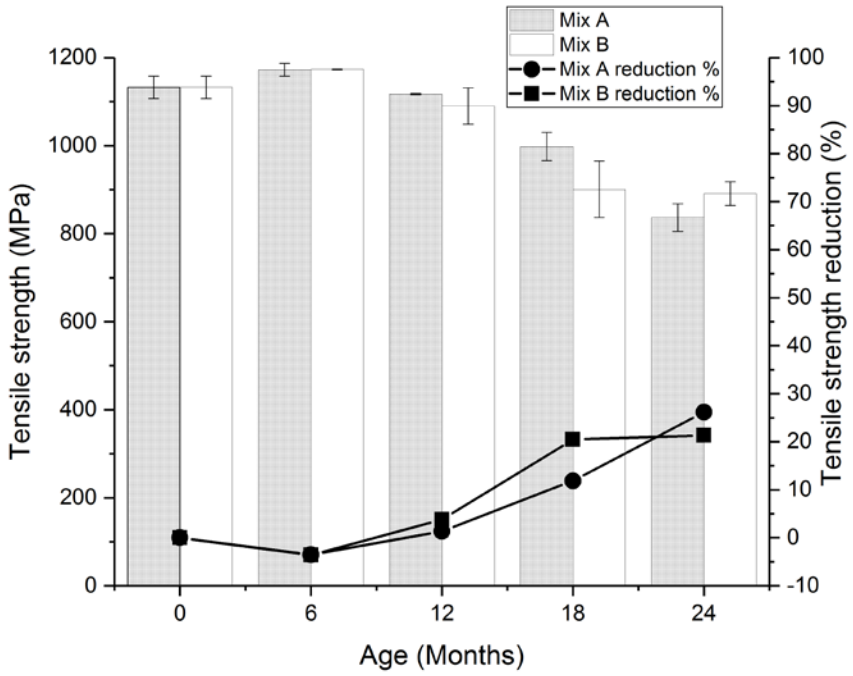

Fig. 3 Tensile strength and reduction percentage (error bars for all the figures are equal to one standard deviation of the average value).

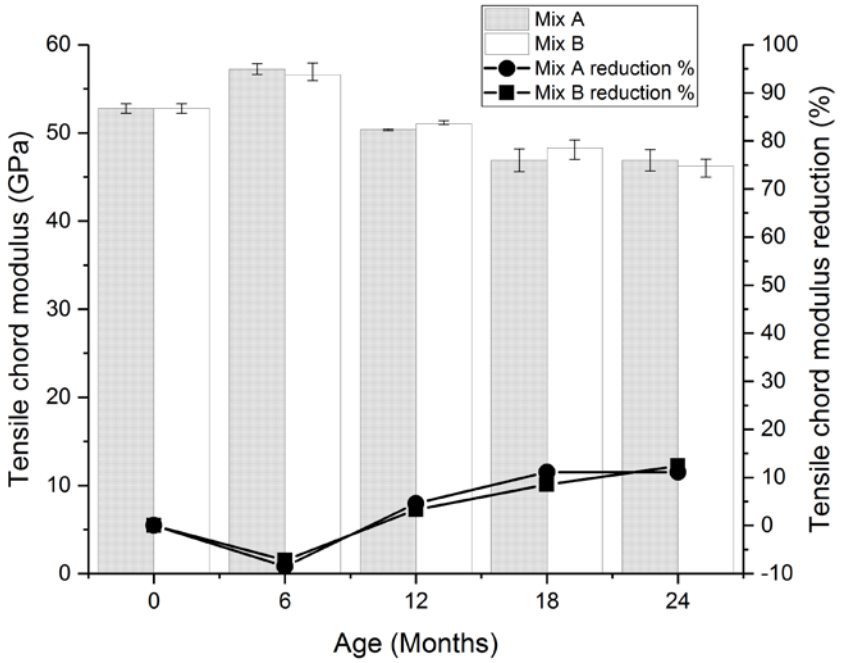

Fig. 4 Tensile chord modulus and reduction percentage.

Fig. 3 shows the change in the tensile strength and reduction percentage (which is the reduction in the value of the property at a certain time with respect to the original value) as a function of immersion time. The chord modulus and reduction percentage as a function of time are shown in **Fig. 4**. One standard deviation on each side of the average is shown by error bars. From these figures, it is apparent that extracted bars from seawater-mixed concrete show comparable performance with the ones from conventional concrete. The tensile strength and chord modulus of both sets of bars slightly increased over the first six months, which may be due to resin crosslinking due to the elevated temperature of the conditioning [41]. Both properties then reduce over time, with reductions of 26 and 21% for extracted bars from conventional and seawater-mixed concrete, respectively, after 24 months exposure. Corresponding reductions in chord modulus are 11 and 12% for extracted

bars from conventional concrete and seawater-mixed concrete, respectively. These findings are in general agreement with literature, though results from the literature show significant variations in the reduction values, depending on bar type, exposure temperature, and exposure solution [23, 24, 26, 42, 43]. El-Maaddawy and co-workers [24] examined seawater-mixed concrete beams reinforced with GFRP and immersed in tap water at 60 °C for 15 months and found that Type I GFRP bars showed better performance than Type II GFRP bars (2 – 15% reduction compared to 19 – 50% reduction). Mortar-wrapped GFRP bars showed 10% reduction in saline solution for 365 days at 50 °C and 16% reduction in tap water at 50 °C for 240 days, indicating that immersion in the saline solution had no more impact on the durability of GFRP bars than immersion in tap water [23, 26]. Others have shown tensile strength reductions till 20% [42, 43]. The tensile modulus of the GFRP bars was not affected by aging in a concrete environment in saline solution or tap water [23, 26], whereas Almusallam and co-workers [42] showed 9% or lesser reduction in tensile modulus for GFRP reinforced specimens immersed in tap water, seawater, and alkaline baths at 50 °C for 18 months.

Apart from the differences in conditioning regimes, the scatter in results obtained by various authors can clearly be attributed to GFRP bar constituents and manufacturing. Bars tested were made of E or E-CR glass and more importantly with different resin systems (never disclosed aside from the generic name of vinyl ester) including undisclosed additives and fillers. Furthermore, manufacturing procedures such as speed of pultrusion and degree of curing affect the quality of the final product. Thus, when referring to a GFRP bar, one is only considering a “class” of products rather than a well-defined system.

Horizontal Shear Strength

GFRP specimens in short beam tests failed in shear (horizontal cracks along the mid-plane of the specimens). **Fig. 5** shows the changes in horizontal shear strength and reduction percentage as a function of time. One standard deviation on each side of the average is shown by error bars. Comparable performance between extracted bars from seawater-mixed concrete and conventional concrete can be observed. The horizontal shear strength decreases as exposure time increases. At the end of 24 months exposure, the reductions in the horizontal shear strength are 21 and 26% for GFRP extracted bars from conventional concrete and seawater-mixed concrete, respectively. These numbers are in general agreement with the literature. Fergani and co-workers [41] examined the effect of sustained load and aggressive environments on the horizontal shear strength and concluded that exposure solution had no significant effect on the strength reduction. Stressed GFRP bars showed better performance with 15% reduction compared to unstressed bars, which showed 25% reduction after 270 days. A reduction of 12% in the horizontal shear strength was reported by Chen and co-workers [13] for GFRP bars embedded in normal concrete and exposed to simulated high performance concrete pore solution at 60 °C. Bakis and co-workers [44] examined the effect of $Ca(OH)_2$ environment on the horizontal shear strength of the GFRP bars and steady loss of strength until one year was observed, at which time the strength loss was 25%.

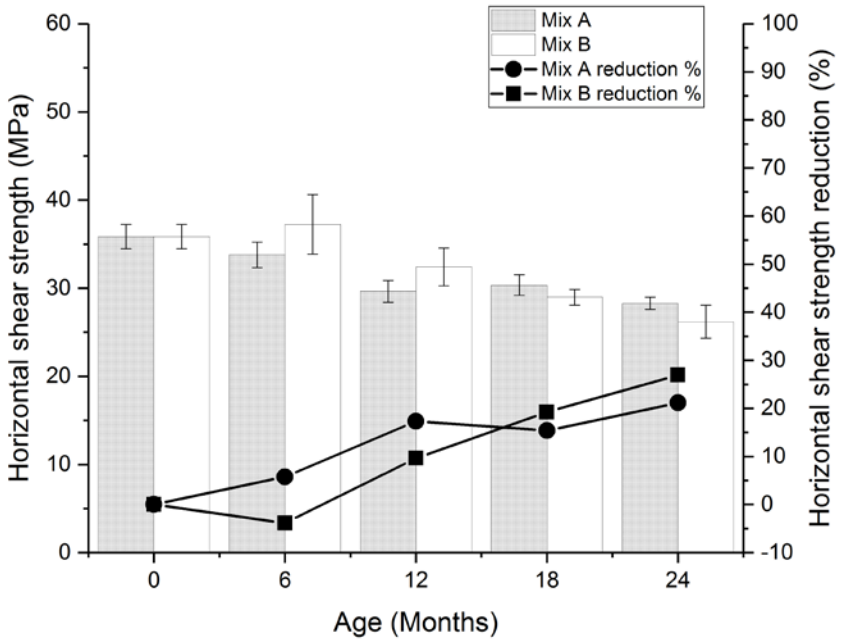

Fig. 5 Horizontal shear strength and reduction percentage.

Transverse Shear Strength

Fig. 6 shows the changes in the transverse shear strength and reduction percentage as a function of time. Error bars show one standard deviation on each side of the average. A similar trend to the horizontal shear strength is observed here. Performance is comparable between GFRP bars extracted from seawater-mixed and conventional concrete. Transverse shear strength decreases over time, and at 24-month exposure, reduction values are 28 and 25% for bars extracted from conventional concrete and seawater-mixed concrete, respectively. It is not possible to compare these results with those from literature, as to the author's best knowledge, there is no study that has examined the effect of concrete environment and saline solution on the transverse shear strength of GFRP bars.

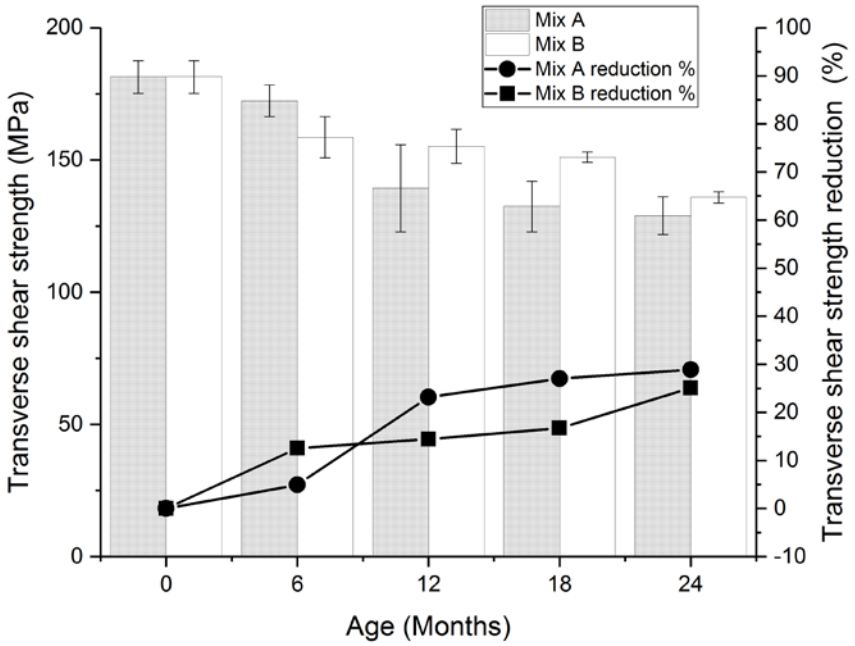

Fig. 6 Transverse shear strength and reduction percentage.

Bond Strength of GFRP Bars

Pull out test specimens failed by slippage. Specimens were split in half to check the failure mode. As shown in **Fig. 7**, the failure occurs at the interface of the double helically twisted wrapped fibers and the bar core. This is due to the lower shear strength at this interface compared to the concrete shear strength. This is consistent with some of technical literature [15, 45]. Control specimens cured in the lab environment and the conditioned specimens (immersed in seawater at 60 °C) exhibited the same failure modes.

Fig. 7 Detail of the extracted GFRP bar after pull out test.

Changes in bond strength and reduction percentage as a function of time is shown in **Fig. 8**. Each error bar shows one standard deviation on each side of the average. Bond strength shows significant deterioration, and after 24 months of immersion in seawater at 60 °C, reduction values are 47 and 55% for conventional and seawater-mixed concrete, respectively. The extent of this deterioration is greater than is typically observed in literature. Bazli and co-workers [46] embedded GFRP bars in four different concrete mixtures and exposed the specimens to seawater at 60 °C for 150 days and observed a reduction in bond strength less than 7%. Park [43] also reported 2.5 – 6% reduction in the bond strength after 300 days immersion in 3% saline solution at 46 °C. Davalos et al. [45] reported 3 – 8% reduction in bond strength of three types of GFRP bars embedded in concrete and immersed in tap water at 60 °C for 90 days. Others have observed a reduction between 8 – 10 % [13, 15]. This variability between the results here and literature could be related to the type of surface enhancement of the GFRP bar as selected by the manufacturer.

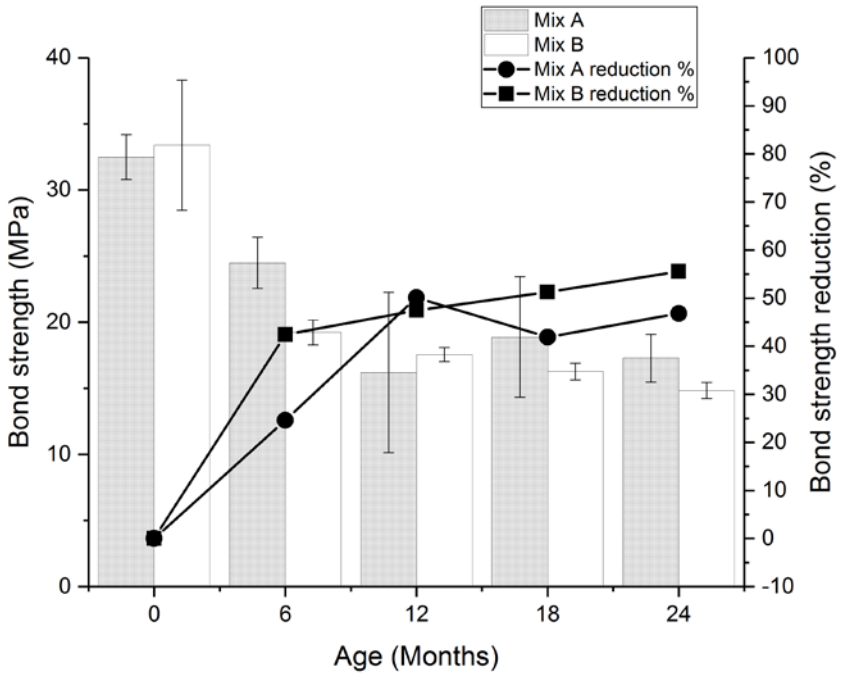

Fig. 8 Bond strength and reduction percentage.

The GFRP bar tested in this study is clearly unsuitable for long-term performance due to the poor quality of the interfacial bond between pultruded core and surface enhancement. This outcome is an additional proof that the attempt to generalize the performance of GFRP reinforcement is not appropriate as each bar presents its own characteristics.

Comparison of GFRP Bar Mechanical Properties

Since a comparable performance was observed between GFRP bars extracted from seawater-mixed and conventional concrete, the average values of the two sets of bars for each mechanical property was graphed and is shown in **Fig. 9**. Tensile modulus shows the least reduction of the tested properties (< 10% at 24 months). Reductions in horizontal and transverse shear strength are comparable and are around 25% at 24 months. While the

reduction in tensile strength is initially lower than the reductions in the horizontal and transverse shear strength, the values at 24 months are comparable. The reduction in bond strength is dramatic and is greater than 50% at 24 months.

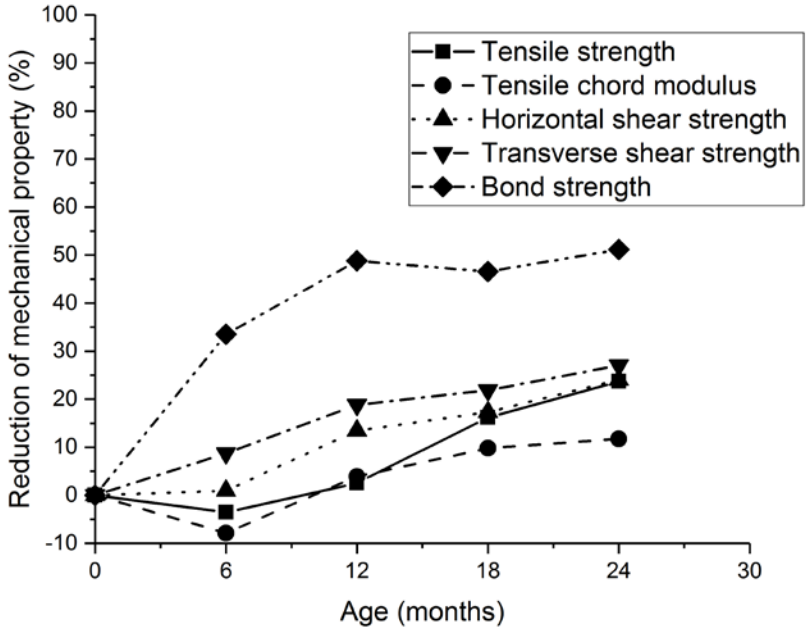

Fig. 9 Average reduction percentage of mechanical properties.

Microstructural Studies

SEM was used to explain degradation mechanisms due to accelerated aging. Micrographs from the pristine bars as shown in **Fig. 10** show areas with large concentrations of defects or voids near the edge (surface) of the bar which are formed during manufacturing. These defects (voids) could provide a pathway for moisture and alkalis which can cause local damage in the form of fiber rupture, resin degradation, and debonding of fiber-resin interface during exposure to saline solutions at high temperatures.

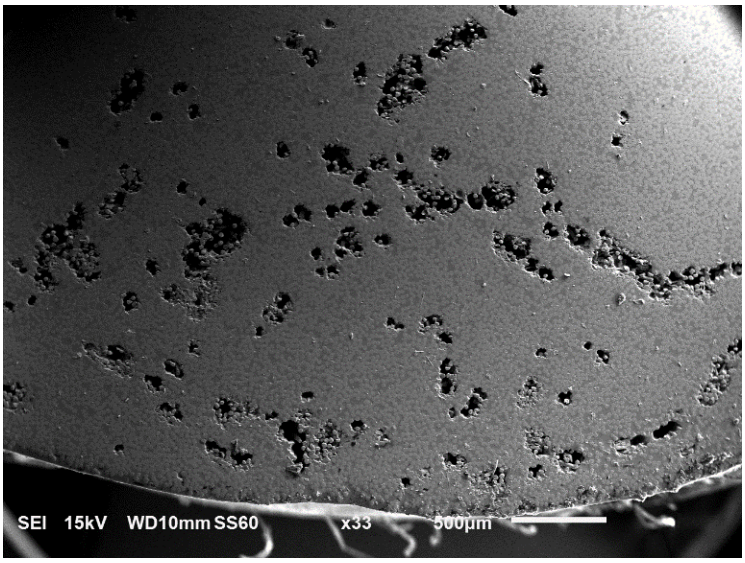

Fig. 10 Representative micrograph of the pristine bar.

An example of such damage close to the edge of the bar is shown in **Fig. 11(a)**, which is taken after 12 months of exposure. In such areas, fiber damage and rupture, fiber-resin debonding, and cracks are clearly observed. The interior regions of the GFRP bars stayed intact over time as shown in **Fig. 11(b)**, taken after 12 months of exposure. Damage in areas close to the edge of the bar and intact interior areas were observed in GFRP bars embedded in conventional and seawater-mixed concretes at all ages of exposure. While it is likely that the extent of damage in areas close to the edge of the bar increases with time, it was not possible to quantify damage change over time using microscopy, due to spatial and temporal variations.

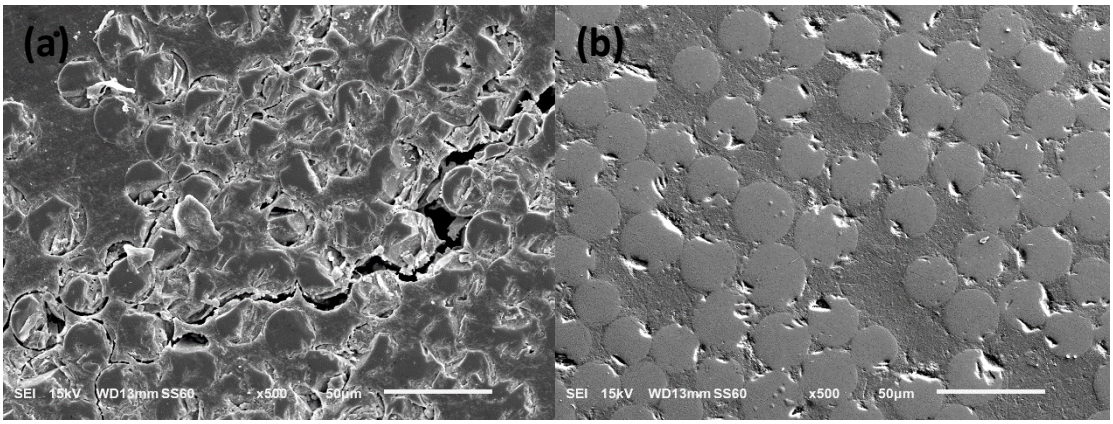

Fig. 11 (a) Representative damaged area near the edge (b) representative intact interior area.

Results were qualitatively similar for embedded bars in seawater-mixed and conventional concrete, explaining the similar reduction seen in both sets of bars. As more areas near the edge are affected, long circumferential cracks form. **Fig. 12** shows three examples of these circumferential cracks at different enlargements. Such crack formation would have a large, negative effect on the bond performance, and explains the large reductions observed in bond strength compared with other mechanical properties. This type of damage mechanism is consistent with some of the technical literature [16, 41, 47, 48].

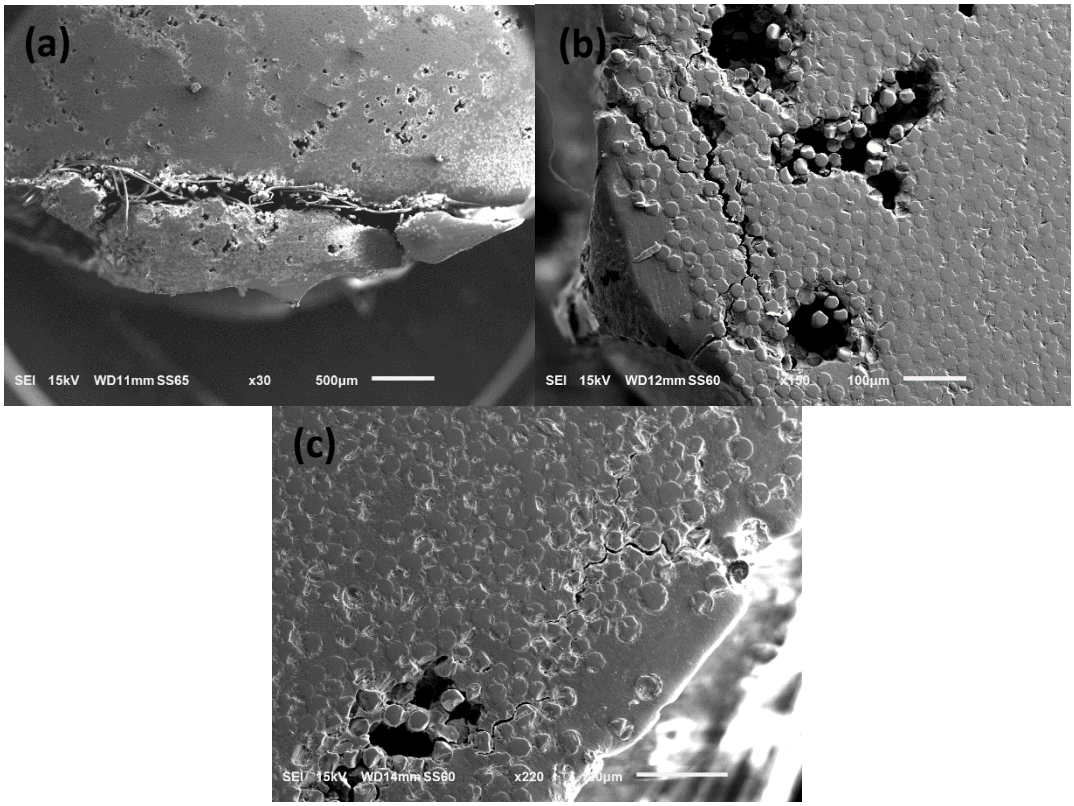

Fig. 12 Representative circumferential cracks near the edge (a) x30 (b) x150 (c) x220 magnification.

EDX was used to find possible patterns in the chemical compositions of the damaged areas. Similar silicon and aluminum contents were observed for GFRP bars extracted from conventional and seawater-mixed concrete. The mass percentages of silicon and aluminum in areas at the bar center on average did not reduce (an increase of 3 % was observed for both elements at 24 months when averaging out bars extracted from conventional and seawater-mixed concrete). On the other hand, for areas close to the edge, silicon and aluminum mass percentages reduced 13% and 20%, respectively (average of bars extracted from conventional and seawater-mixed concrete after 24 months of immersion in seawater at 60 °C). These results were obtained from EDX performed on at least ten randomly chosen “bulk” areas chosen at 500x magnification, they suggest that the glass content (fiber

content) is reducing near the bar edge, but not at the bar center. This is likely due to glass dissolution or deterioration due to the presence of moisture, alkalis and high temperature. This is consistent with literature showing that damaged fibers show significantly lower silicon contents compared with undamaged fibers [48].

Conclusions

The following conclusions can be drawn from this study:

a) Extracted GFRP bars from the conventional and seawater-mixed concrete showed comparable performance indicating that using seawater as mixing water has no significant effect on the durability of GFRP bars.
b) Tensile and shear strength properties showed a moderate reduction after 24-month immersion in seawater at 60 °C. Tensile strength decreased by 21 – 26%, tensile modulus by 6 – 12%, horizontal shear strength by 21 – 26%, and transverse shear strength by 25 – 28%.
c) The bond strength showed the highest degradation, with 47 and 55% reductions for bars extracted from conventional and seawater-mixed concrete, respectively.
d) Micrographs showed a large number of defects (voids) near the edge of the bars, which may have been formed during manufacturing. These defects (voids) provide a pathway for alkalis, which can cause local damage in the forms of fiber disintegration and de-bonding between fibers and resin matrix. More fibers are affected over time, leading to circumferential cracks near the edge. This leads to a degradation of the edge (surface), which explains the large reduction in the bond strength, compared to other mechanical properties.

Unless industry develops consensus standards on composition, manufacturing and type of surface enhancement for bond with concrete, each commercially available GFRP bar system will have to be thoroughly tested in order to assess its performance and long-term durability. Generic statements about “all” bars are not possible. It should be noted that the bars tested in this study are categorized as the first generation of the GFRP bars. As manufacturing techniques have improved over time, the quality and durability of bars also improved. Research has shown that the second generation of the GFRP bars are significantly more durable in terms of mechanical properties when exposed to the same accelerated aging [49].

CHAPTER 3

COMPRESSIVE STRENGTH DEVELOPMENT OF CONCRETE MIXED WITH SEAWATER SUBJECT TO DIFFERENT CURING REGIMES

Background

Literature has addressed the strength development of concrete mixed with seawater. Results typically show higher early age strength [8, 50-61]; however, the long-term strength have shown inconclusive or contradictory results. Some researchers show a slight reduction [52, 54], while others show comparable or higher long-term strength for seawater-mixed concrete [60, 61]. Mohammed et al. [50] studied the compressive strength of seawater-mixed concrete after 20-year exposure to a simulated tidal pool and concluded that the compressive strength of concrete was independent of the type of mixing water. Similar observations were reported by Otsuki et al. [62].

Mixing concrete with seawater may also affect the microstructure and hydration products. Ghorab et al. [8] observed early-age gypsum precipitation; however, this was not observed at later ages, and the types and amounts of phases formed after one year were unaffected by the water type. Work on cement pastes has shown that a certain amount of chlorides could be incorporated in the C-S-H; however, calcium hydroxide and bound water amounts were not affected by the use of seawater as mixing water [63]. The use of seawater slightly increases the density and decreases the porosity and permeability of the concrete [51].

A synergistic effect between supplementary cementitious materials and seawater has been shown. Shi et al. [64] and Li et al. [65] showed that seawater-mixed concrete with 5%

metakaolin addition increased the 28-day compressive strength by 52% compared to concrete mixed with fresh water and no metakaolin. This was attributed to the acceleration of the pozzolanic reaction of metakaolin by seawater and a refinement of the pore structure in the seawater-mixed concretes with metakaolin. Seawater was proposed to be an accelerator for fly ash [66] and for ground granulated blast furnace slag [57]. This accelerating effect is due to the higher amount of available calcium hydroxide for the pozzolanic reaction, which is also caused by higher extent of cement hydration in the presence of seawater.

While several studies have looked at the long-term performance of concrete mixed with seawater, little research has been done on a direct comparison of conventional concrete and seawater-mixed concrete in various environments, and this is the objective of this study. In addition, a set of specimens exposed to one curing condition (immersion in seawater at 60 °C [140 °F]) is studied using thermogravimetric analysis (TGA), energy-dispersive X-ray spectroscopy (EDX), electrical resistivity, water absorption, and density measurements in order to explain the strength development of seawater-mixed concrete under certain curing regimes.

Experimental Investigation

Materials

A type II cement meeting the requirements of ASTM C150/C150M-18 [29] and a type F fly ash conforming to ASTM C618-17a [30] were used in this study. Their oxide compositions and the phase composition of the cement are listed in **Table 4**. Tap water and seawater from Key Biscayne Bay (FL) were used as mixing water, with chemical

composition (determined by inductively coupled plasma atomic emission spectroscopy [ICP-AES]) as shown in **Table 5**. Further details are presented elsewhere [31]. Miami oolite with a nominal maximum size of 25 mm (1 in.) was used as the coarse aggregate and silica sand as the fine aggregate.

Table 4 Composition of the cement and fly ash

Composition	**Mass (%)**	
	Type II cement	**Fly ash**
SiO_2	20.50	46.80
Al_2O_3	4.90	19.30
Fe_2O_3	3.90	18.99
CaO	64.40	5.50
MgO	0.90	0.90
SO_3	2.60	2.23
$Na_2O_{eq.}$	0.25	0.88
Loss on ignition	2.10	3.10
Bogue Phase Calculation*		
C_3S	60	-
C_2S	14	-
C_3A	7	-
C_4AF	12	-

Table 5 Chemical compositions of tap water and seawater used in concrete mixtures

Ions	Concentration (ppm)	
	Tap Water	**Seawater**
Calcium	90	389
Chloride	44	18759
Iron	-	0.5
Potassium	6	329
Magnesium	6	1323
Sodium	26	9585
Sulfate	8	2489
Nitrate	1	0.1

Concrete mixtures

Two different concrete mixtures with water-to-cementitious materials ratio (w/cm) of 0.40 were cast: Mix A is the reference conventional concrete and Mix B is the seawater-mixed concrete. The mixture proportions of Mix B are identical to those of Mix A, but fresh water is substituted with seawater from Key Biscayne Bay, Florida. **Table 6** shows the mixture proportions. Concrete was mixed using a drum mixer. Aggregate moisture content was measured and the amount of mixing water was adjusted accordingly. Aggregates were added into the mixer with approximately one-third of the mixing water and mixed for three minutes, after which the cementitious materials and the remaining water were added and mixed for three more minutes. Mixing was paused for two minutes while the sides of the mixing drum were scraped. Chemical admixtures were added as applicable, and the mixture was mixed for a final duration of three minutes. Slump, density

and air content of the fresh concrete were measured in accordance with ASTM C143/C143M-15a [67], ASTM C138/C138M-17a [68], and ASTM C231/C231M-17a [69], respectively. Further details about the concrete are presented elsewhere [31]. The time of setting on the corresponding cement pastes was also measured by Vicat needle per ASTM C191-18 [70]. The paste samples were mixed using mechanical mixer per ASTM C305-14 [71]. Mixing water was placed in the mixing bowl to which cement was added and left to absorb water for 30 seconds. Then, the mixture was mixed at slow speed (140 ± 5 r/min) for 30 seconds. The mixer was paused for 15 seconds in order to scrape the sides of the bowl, after which the mixture was mixed for 60 seconds at medium speed (285 ± 10 r/min).

Table 6 Mixture proportions

Material	**Units**	**Mix A**	**Mix B**
Portland cement I-II (MH)	kg/m^3 (lb/yd^3)	332 (559)	332 (559)
Fly ash	kg/m^3 (lb/yd^3)	83 (140)	83 (140)
Tap water	kg/m^3 (lb/yd^3)	168 (283)	-
Seawater	kg/m^3 (lb/yd^3)	-	168 (283)
Coarse aggregate	kg/m^3 (lb/yd^3)	1038 (1750)	1038 (1750)
Fine aggregate	kg/m^3 (lb/yd^3)	612 (1032)	612 (1032)
Set retarding admixture	ml/m^3 (gal/yd^3)	-	830 (0.2)
Air-entraining admixture	ml/m^3 (gal/yd^3)	310 (0.1)	310 (0.1)

Curing Regimes and Compressive Strength

Concrete cylinders with dimensions of 100 x 200 mm (4 x 8 in.) were cast per ASTM C39/C39M-18 [72] using conventional concrete (Mix A) and seawater-mixed concrete (Mix B). These samples were moist cured in a fog room (100% relative humidity and temperature of 23 ± 1 °C [73.4 ± 2 °F]) for 28 days. Early-age compressive strength was tested at 3, 7, and 28 days of moist curing (testing was performed as described below using three repetitions). The effect of different curing regimes was then examined by monitoring the compressive strength after exposing the concrete cylinders to four different environments: subtropical environment, tidal zone, moist curing, and seawater at 60 °C (140 °F). The curing regimes were selected considering possible environments that seawater-mixed concretes could be exposed to in real life. These environments are described below and shown in **Fig. 13**:

Fig. 13 Different curing regimes (a) subtropical environment; (b) tidal zone; (c) moist curing; (d) immersed in seawater at 60 °C (140 °F).

Subtropical environment: Specimens were placed outdoors in Coral Gables, FL with an average temperature range of 15 – 33 °C (59 – 91.4 °F) and monthly average precipitation of 131 mm (5 in.) [73].

Tidal zone: The tidal zone utilized in this study is located at Key Biscayne Bay, FL with the average water temperature range of 23 – 30 °C (73.4 – 86 °F) [73] and salinity range of 1.7 – 3.1% [74]. The specimens were placed such that they experienced wetting and drying cycles during and high and low tides, respectively.

Moist curing: Moist curing was done in a fog room with 100% relative humidity and a temperature of 23 ± 1 °C (73.4 ± 2 °F). This was considered to be the control environment.

Seawater at 60 °C (140 °F): Samples were immersed in seawater at 60 °C (140 °F) in a tank filled with the same seawater that was used for mixing (**Table 5**). A constant temperature was maintained using an immersion heater. Seawater was slowly circulated in and out of the tank to provide a constant exposure to seawater of fixed chemical composition. This exposure can be considered as an accelerated curing regime, as the elevated temperature increases the rate of hydration [75] and the rate of potential chemical degradation [76, 77].

Concrete compressive strength was tested after 6, 12, 18, 24 months. Three concrete specimens for each mixture were extracted from exposure sites, surface dried, and brought to the laboratory. Sulfur capping was applied on all the samples which were left at ambient temperature inside the lab for 8 to 12 hours before testing.

Concrete exposed to seawater at 60 °C (140 °F) is expected to show some reduction in strength due to leaching effects. In order to quantify the leaching and its effects on the strength development, further testing was performed on samples immersed in seawater at 60 °C (140 °F) for 24 months.

Thermogravimetric Analysis (TGA)

Thermogravimetric analysis (TGA) was performed on concrete samples exposed to seawater at 60 °C (140 °F) after 24 months. Concrete samples were extracted from seawater, surface dried using a towel, and then broken into pieces. Pieces were collected from near the surface and the bulk of these specimens. These pieces were gently crushed with pestle separating out the coarse and fine aggregate. The samples were then sieved through a 75 μm (2.95×10^{-3} in.) sieve to ensure that as much as possible cement paste was

used to perform the TGA (although small portion of sand could still be present). In order to obtain a representative value, five samples from each location were tested for both mixes. The TGA (TGA 55, TA instruments) was performed in an inert nitrogen atmosphere by increasing the temperature at the rate of 10 °C (18 °F) per minute from 23 °C (73.4 °F) to 1000 °C (1832 °F). The tangent method was used to quantify the amount of calcium hydroxide present in the sample [78].

Energy-Dispersive X-ray Spectroscopy (EDX)

Energy-dispersive X-ray (EDX) spectroscopy was used to investigate potential ingress and egress of various ions from and into the concrete after being cured in seawater at 60 °C (140 °F) for 24 months. Representative samples were taken from near the surface and the bulk of concrete cylinders (in the same manner as was done for TGA testing) and impregnated in hot acrylic resin at a temperature of 120 °C (248 °F) and 50 mbar (0.73 psi) pressure. After the acrylic resin hardened, samples were polished using different grit levels (i.e., 180, 300, 600 and 1200) of sand paper using grinding and polishing equipment. The specimens were then fine polished using a wet-polishing agent and 3 μm (1.18×10^{-4} in.) and 1 μm (3.94×10^{-5} in.) polycrystalline diamond paste. Prior to imaging, specimens were placed in a vacuum oven at 50 °C (122 °F) for 24 h to remove any moisture introduced during polishing and then gold-coated prior to imaging. EDX was performed on randomly chosen near-surface or bulk specimens from the concretes. Analysis was performed on at least 10 different spots on the sample. While the exact parameters used for testing varied, typical settings are: Voltage = 20 kV, Working Distance = 10 mm (0.4 in.), Spot Size = 65, Magnification = 1500x, and Dead Time = 20 – 30 %.

Electrical Resistivity and Formation Factor

Electrical resistivity and formation factor (a parameter that describes the microstructure and transport properties of the concrete) [79, 80] of the concrete cylinders made with conventional concrete and seawater-mixed concrete were measured after immersion in seawater at 60 °C (140 °F) for 24 months. Concrete cylinders were removed from the storage chamber and wiped with a cloth to achieve surface-dry conditions. Two stainless steel plate electrodes with a diameter of 102 mm (4 in.) were used with two pieces of sponge saturated with seawater between specimen and plate electrodes to ensure an electrical connection. The resistivity of the concrete cylinders was measured using a bulk resistivity meter with a frequency of 1 kHz at 23 ± 1 °C (73.4 ± 2 °F) [81]. Although resistivity measurements are a good indicator of the concrete quality, in order to have a better understanding of the porosity and the pore connectivity, the chemistry of the pore solution should be considered. To this end, the formation factor was determined through normalization of the bulk electrical resistivity by the pore solution resistivity. Since the storage solution (seawater) was being circulated and replaced regularly and the specimens were immersed for a long period of time at high temperature (60 °C [140 °F] for 24 months), it was assumed that the concentration of the pore solution in the concrete was the same as the storage solution (seawater) [82]. In addition, it was assumed that the specimens are fully saturated after exposure to these storage conditions. Formation factor (F) of the concrete specimens cast with conventional concrete and seawater-mixed concrete was calculated from Equation (1) [81]:

$$F = \frac{\rho_{SAT}}{\rho_{ps-SAT}} \quad (1)$$

where, ρ_{SAT} is the electrical resistivity of the concrete specimen (Ω-m) (Ω-in) and ρ_{ps-SAT} is the electrical resistivity of the pore solution (Ω-m) (Ω-in). The value of ρ_{ps-SAT} is the same as the resistivity of the seawater which was estimated from OH^-, K^+, and Na^+ concentrations using the method proposed by Snyder et al. [83].

Water Absorption and Dry Density

Water absorption of the concrete cylinders made with conventional concrete and seawater-mixed concrete was measured after immersion in seawater at 60 °C (140 °F) for 24 months. It was assumed that the specimens are fully saturated after 24-month immersion. Three specimens from each mixture were removed for the storage chamber and wiped with a cloth to achieve saturated surface-dry conditions, and then dried in the oven at 105 °C (221 °F) for 48 hours. Water absorption was calculated from Equation (2):

$$Water\ absorption\ (\%) = \frac{Saturated\ weight - Oven\ dry\ weight}{Oven\ dry\ weight} \times 100 \quad (2)$$

The oven dry weight was also used to calculate the dry density of these samples. The water absorption and dry densities are used as indicators of ingress of seawater and leaching of material into seawater, respectively.

Experimental Results and Discussion

Fresh Properties

Fresh properties of the concrete and setting times of the cement pastes mixed are shown in **Table 7**. Slump, density, and air content of conventional concrete and seawater-mixed concrete are similar. The same trend has been reported by other researchers [51, 58]. Setting times were affected by the use of seawater. Cement paste mixed with seawater showed an earlier setting by approximately 60 minutes, which was also qualitatively observed during casting concrete specimens. This is due to the acceleration of the cement hydration by the chlorides in seawater [8, 51, 57]. When accelerated setting is not desirable, set times may be controlled by using set retarding admixtures [59].

Table 7 Fresh properties and setting time

Mixture	Slump, mm (in.)	Density, kg/m^3 (lb/ft^3)	Air content (%)	Setting time (minutes)	
				Initial	Final
Mix A	100 (4)	2350 (146.7)	1.3	255	435
Mix B	95 (3.75)	2359 (147.3)	1.0	195	375

Early-age Compressive Strength

Fig. 14 shows the compressive strength evolution in the first 28 days. The figure also shows the percentage difference between the conventional concrete and seawater-mixed concrete ([Mix B – Mix A]/Mix A, expressed as a percentage). In this figure and in similar figures in the paper, the error bars on each side represent one standard deviation of the average. Concrete mixed with seawater showed higher compressive strength after 3 and 7

days by 7.5% and 6%, respectively. This is due to accelerating effect of chloride on the early age hydration [8, 57]. This difference decreases with time, as both mixtures show comparable performance after 28 days (at this age, seawater-mixed concrete shows 1% higher strength). The same trend was observed by other researchers [8, 50-61].

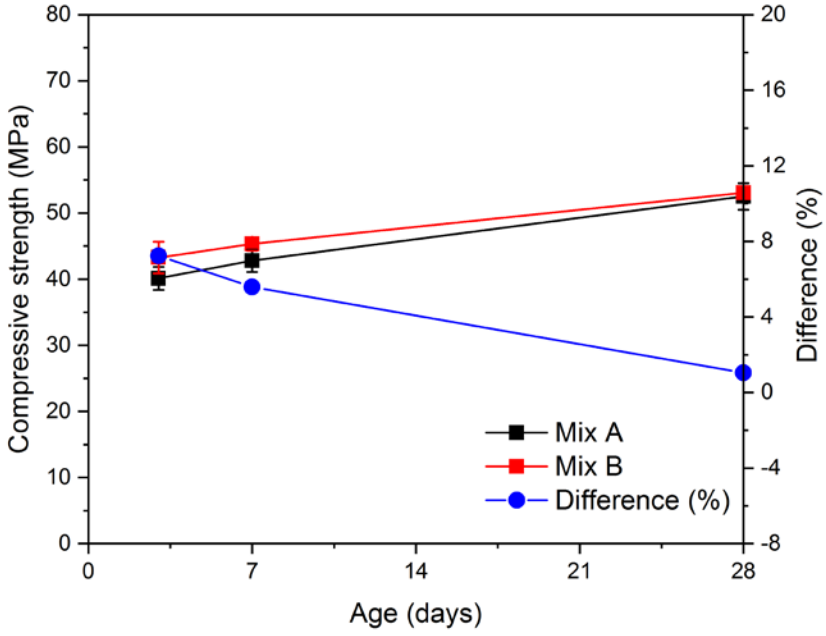

Fig. 14 Early-age compressive strength and percentage difference. (1 MPa = 145.038 psi).

Compressive Strength

Subtropical environment: **Fig. 15** shows the compressive strength development and the percentage difference of the conventional concrete and seawater-mixed concrete cylinders exposed to the subtropical environment of Coral Gables, FL. The strength of the seawater-mixed concrete increases continuously whereas the strength of the conventional concrete increases till 12 months and subsequently slightly reduces. In general, the strength development of the concrete mixtures is comparable; however, at 24 months exposure to

ambient temperature, the seawater-mixed concrete shows a 7% higher compressive strength than the conventional concrete. This is likely explained by the accelerating effect of seawater on the fly ash reaction [66]. It is possible that in these conditions, seawater-mixed concrete has a greater degree of pozzolanic reaction of the fly ash, leading to greater strength at later ages. These results are in agreement with literature. Abrams who tested concrete cylinders after 28 months air curing at 20 °C (68 °F) [53] and Jensen and Pratt who tested cement and fly ash blended paste specimens for 12 months at 20 °C (68 °F) [66] both showed similar or slightly higher strength development in seawater-mixed concrete.

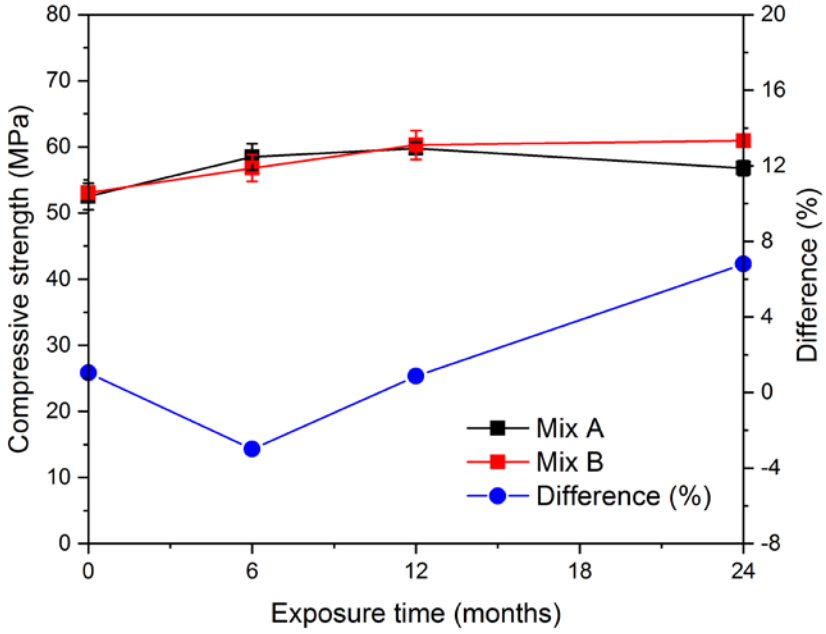

Fig. 15 Compressive strength and percentage difference in subtropical environment of Coral Gables, FL for 24 months (1 MPa = 145.038 psi).

Tidal zone: **Fig. 16** shows the compressive strength development and the percentage difference of the conventional concrete and seawater-mixed concrete cylinders exposed to the tidal zone. The strength of the concrete mixed with seawater increases continuously

whereas the strength of the conventional concrete increases till 6 months and subsequently decreases. At 24 months exposure to the tidal zone, the concrete mixed with seawater shows a 10% higher compressive strength than the conventional concrete. One reason for the better performance of seawater-mixed concrete could be the greater degree of pozzolanic reaction of the fly ash, leading to greater strength at later ages [66]. Another possible reason is lower leaching in the seawater-mixed concrete compared to conventional concrete when exposed to the tidal zone. The difference between the pore solution ionic concentration of the conventional concrete and surrounding seawater could lead to the leaching of alkalis and calcium hydroxide from the sample which can cause an increase in the porosity and reduce the strength [82]. The pore solution ionic concentrations in the seawater-mixed concrete are more similar to the surrounding seawater (as an example, sodium and chloride concentrations in pore solutions extracted from a paste mixture similar to Mix A at 28 days are 0.1 M and 0.0 M, corresponding values for a mixture similar to Mix B are 0.7 M and 0.5 M, while values for seawater are 0.5 M and 0.6 M). Therefore, leaching in the seawater-mixed concrete is likely reduced [63]. Results from literature for tidal zone exposure are contradictory. Mohammed et al. [50] showed similar or higher compressive strength for the concrete cast using cement and fly ash blends mixed with seawater compared with conventional concrete exposed to simulated tidal zone for 15 years. Otsuki et al. [62] also reported about 5% higher compressive strength for the concrete specimens mixed with seawater without any supplementary cementitious materials exposed to tidal zone for 20 years. On the other hand, higher compressive strength by 5 – 10% for concrete specimens mixed with fresh water without any supplementary cementitious materials was reported by Kaushik and Islam [59] after

exposure to alternate wetting and drying cycles in simulated tidal zone for 18 months. This contradiction could be possibly due to variability in the used materials. Nevertheless, when one considers the effect of leaching, it is intuitive that seawater-mixed concrete shows a better compressive strength development.

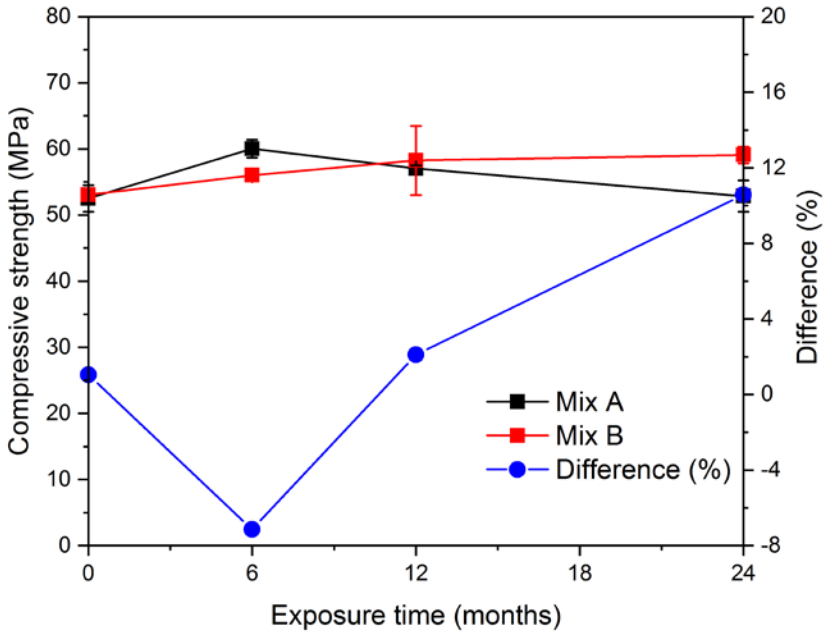

Fig. 16 Compressive strength and percentage difference in tidal zone in Key Biscayne, FL for 24 months (1 MPa = 145.038 psi).

Moist curing: **Fig. 17** shows the compressive strength development and percentage difference of the conventional concrete and seawater-mixed concrete cylinders exposed to moist curing. Both concretes show an increase in strength till 6 months and then a subsequent decrease. The strength development of the concrete mixtures is comparable, however, at 24 months exposure to moist curing, the concrete mixed with seawater shows a 4% lower compressive strength than the conventional concrete. The same ideas regarding leaching are also applicable in this context. In a moist curing condition, the surface of the

concrete samples is covered with water. There is a larger difference in ionic strengths between water and the seawater-mixed concrete when compared with conventional concrete (as an example, ionic strengths of pore solutions extracted from paste mixtures similar to Mix A and Mix B at 28 days are approximately 0.3 M and 1.0 M, respectively) [63]. This may result in leaching of calcium hydroxide and alkalis from the seawater-mixed concrete, which may alter the porosity and microstructure [84, 85], and result in a reduction of the strength. These results are in agreement with literature. Abrams [53] showed 12 – 20% reduction in the compressive strength of the concrete mixed with seawater cured in moist room for 28 months compared with conventional concrete. Etxeberria et al. [51] showed an 8% reduction for concrete mixed with seawater compared to conventional concrete when exposed to a moist room for 12 months and Islam et al. [86] showed 5 – 10% reduction after 6 months curing in fresh water. The above results are for concrete made without supplementary cementitious materials and they show a greater reduction in seawater-mixed concrete strength (compared to conventional concrete) that the one observed here. This is possibly due to the enhanced pozzolanic reaction of fly ash somewhat mitigating the strength reduction due to leaching [66] or a reduction in the extent of calcium hydroxide leaching in the presence of fly ash [87].

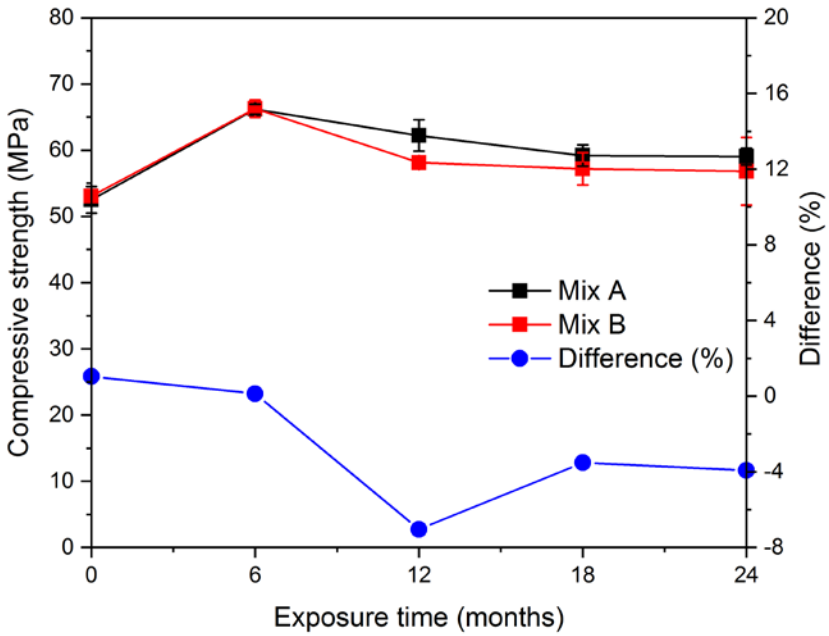

Fig. 17 Compressive strength and percentage difference in moist curing for 24 months (1 MPa = 145.038 psi).

Seawater at 60 °C (140 °F): **Fig. 18** shows the compressive strength development and percentage difference of the conventional concrete and seawater-mixed concrete cylinders exposed to seawater at 60 °C (140 °F). Both concretes show an increase in strength till 6 months and then a subsequent decrease. In general, seawater-mixed concrete shows higher compressive strength development and values at 24 months were 14% higher than conventional concrete. The leaching mechanism explained for the tidal zone also likely applies in this scenario. The higher temperature and the submersion may cause a greater extent of leaching, which explains the greater difference in strength between conventional concrete and seawater-mixed concrete (as compared to the tidal zone). **Fig. 19** shows a layer of leached material covered the surface of a concrete cylinder cast with conventional concrete and immersed in seawater at 60 °C (140 °F) for 24 months. Strength loss due to

leaching has been suggested by other researchers [66] for conventional concrete exposed to seawater at room temperature. Jensen and Pratt [66] immersed cement and fly ash pastes mixed with seawater and distilled water in seawater at 8 °C (46 °F) for 12 months and observed that seawater mixed specimens showed higher compressive strength due to the leaching of calcium hydroxide in pastes mixed with distilled water when cured in seawater. The same trend was noted by Lim et al. [88] in which mortar specimens with 20% fly ash replacement were immersed in seawater for 5 months. On the other hand, Weigan [52] reported 20% lower compressive strengths for the concrete specimens mixed with seawater compared with specimens mixed with fresh water after curing in seawater for 3 months. Islam et al. [86] showed 1 – 7% reduction after 3 months curing in seawater when seawater was used as the mixing water. Concrete samples mixed with seawater and supplementary cementitious materials show better performance than samples without supplementary cementitious materials, showing the synergistic effect of seawater and supplementary cementitious materials [50, 62].

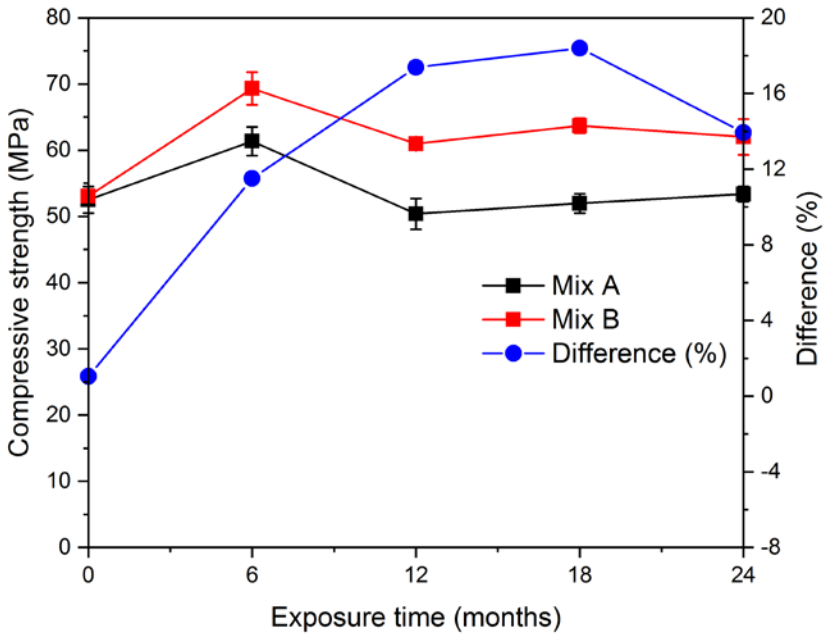

Fig. 18 Compressive strength and percentage difference in seawater at 60 °C (140 °F) for 24 months (1 MPa = 145.038 psi).

Fig. 19 A layer of leached material covered the surface of a concrete cylinder cast with conventional concrete (Mix A) after immersion in seawater at 60 °C (140 °F) for 24 months.

Comparison of compressive strength development in different curing regimes: Conventional concrete performed well when cured in moist room or outside the lab. However, the lowest compressive strengths for conventional concrete were recorded at 24 months of curing in tidal zone and moisture room. As postulated earlier, the differences between the pore solution ionic concentration of the conventional concrete and surrounding seawater could lead to the leaching of alkalis and calcium hydroxide from the sample which can cause an increase in the porosity and negatively affect the strength. On the other hand, seawater-mixed concrete cured in seawater at 60 °C (140 °F) had the highest compressive strength at 24 months compared with other curing regimes and the lowest

compressive strength was in moist curing conditions. The leaching mechanism due to the large difference in ionic strengths between pore solution and curing environment can also explain the relatively inferior performance of the seawater-mixed concrete in the moist room. Analysis of variance (ANOVA) shows no significant difference between the compressive strength of conventional and seawater-mixed concrete at 24 months considering all curing regimes.

Thermogravimetric Analysis (TGA)

Table 8 shows the calcium hydroxide content near the surface and in the bulk of the conventional concrete and seawater-mixed concrete specimens after exposure to seawater at 60 °C (140 °F) for 24 months. The amounts of calcium hydroxide near the surface and in the bulk of the concrete specimens cast with seawater-mixed concrete are 4.87 g/100 g paste (0.17 oz./3.5 oz. paste) and 4.61 g/100 g paste (0.16 oz./3.5 oz. paste), respectively. However, lower amounts of calcium hydroxide, 2.92 g/100 g paste (0.10 oz./3.5 oz. paste) and 4.23 g/100 g paste (0.15 oz./3.5 oz. paste) were measured for the conventional concrete near the surface and in the bulk, respectively. Significantly lower calcium hydroxide content near the surface of the conventional concrete confirms the hypothesis that ionic concentration gradient between the pore solution and surrounding environment causes the leaching and negatively affect the compressive strengths. As the unaltered calcium hydroxide contents are unknown, the extent of leaching is not possible to determine accurately, however, the large difference (30%) in values between the surface and the bulk for the conventional concrete suggests that the calcium hydroxide leaching is significant. Jensen and Pratt [66] reported similar calcium hydroxide leaching in paste specimens

mixed with distilled water and cured in seawater at 8 °C (46 °F) for 365 days and suggested that it was responsible for strength loss in these specimens.

Table 8 Calcium hydroxide content near the surface and in the bulk of the concrete specimens exposed to seawater at 60 °C (140 °F) for 24 months.

Mixture	Calcium hydroxide content, g/100 g paste (oz./3.5 oz. paste)			
	Near the surface	Standard deviation	Bulk	Standard deviation
Mix A	2.92 (0.10)	0.70 (0.02)	4.23 (0.15)	0.52 (0.02)
Mix B	4.87 (0.17)	1.08 (0.04)	4.61 (0.16)	0.85 (0.03)

Energy-Dispersive X-ray spectroscopy (EDX)

EDX was used to find patterns in the chemical compositions of the bulk and areas near the surface of the conventional concrete and seawater-mixed concrete specimens after exposure to seawater at 60 °C (140 °F) for 24 months. Similar chloride contents were observed in the bulk and near the surface of both concrete mixtures (1.72 – 1.87%). The lack of a significant gradient between the chloride contents in the bulk and surface and the similar values between the two concrete specimens suggests that the chloride has fully diffused into the conventional concrete specimens due to ionic gradients between the initial pore solution and seawater and the exposure temperature (60 °C) (140 °F).

Electrical Resistivity and Formation Factor

Table 9 shows electrical resistivity and formation factor values of the conventional concrete and seawater-mixed concrete specimens after exposure to seawater at 60 °C (140

°F) for 24 months. The electrical resistivity of seawater-mixed concrete (540.2 Ω-m) (21268 Ω-in) was 33% higher than the electrical resistivity of the conventional concrete (406 Ω-m) (15984 Ω-in). These results are in agreement with the compressive strength results (16% greater compressive strength for seawater-mixed concrete) and confirm that the seawater-mixed concrete performs better when immersed in seawater at 60 °C (140 °F). These results are broadly similar to values with literature which suggests electrical resistivity values of 300 – 1000 Ω-m (11811 – 39370 Ω-in) for concrete mixtures with 25% or more fly ash at ages of 10 years or greater [89]. An exact comparison is not possible as data does not exist for seawater-mixed concretes or for concretes immersed in seawater at 60 °C (140 °F). The formation factor of these concretes can be determined through normalization of the bulk electrical resistivity by pore solution resistivity. Due to the sufficiently long storage time and the use of circulating seawater during the storage, it is assumed that there is a complete ingress of the seawater into the concrete, or, in other words, that the pore solution in both concretes is the seawater. A method proposed by Snyder et al. [83] was used to calculate the resistivity of seawater based on its composition. This gives the resistivity of the seawater as 0.222 Ω-m (8.74 Ω-in). Formation factor can then be calculated for both concrete mixtures. Formation factor of seawater-mixed concrete (2422) was 33% higher than that of the conventional concrete (1829). In a related study, the electrical resistivity of pore solutions extracted from paste mixtures similar to Mix A and B at 91 days was determined to be 0.147 Ω-m (5.79 Ω-in) and 0.08 Ω-m (3.15 Ω-in), respectively [63]. If an incomplete extent of solution ingress is assumed, then the pore solution resistivity values of Mix A and Mix B would be between 0.147 – 0.222 Ω-m (5.79

– 8.74 Ω-in) and 0.08 – 0.222 Ω-m (3.15 – 8.74 Ω-in), which suggests that the difference in the formation factors would be even greater than 33%.

Table 9 Resistivity measurements and formation factor

Mixture	Resistivity, Ω-m (Ω-in)	Standard deviation, Ω-m (Ω-in)	Formation Factor
Mix A	406.0 (15984)	57.1 (2248)	1829
Mix B	540.2 (21268)	142.4 (5606)	2433

Water Absorption and Dry Density

Table 10 shows water absorption and dry density values of the conventional concrete and seawater-mixed concrete after 24 months immersion in seawater at 60 °C (140 °F). In that time period, conventional concrete absorbed 3.5% water (seawater), which is larger than the corresponding value for seawater-mixed concrete (2.8%). This shows a greater extent of seawater ingress in the conventional concrete than the seawater-mixed concrete. The dry densities of the seawater-mixed concrete (2350 kg/m^3) (146.7 lb/ft^3) is greater than conventional concrete (2312 kg/m^3) (144.3 lb/ft^3). When compared with the fresh density (**Table 7**), conventional concrete showed a 38 kg/m^3 (2.36 lb/ft^3) reduction, however, seawater-mixed concrete showed a 9 kg/m^3 (0.56 lb/ft^3) reduction, showing that the leaching of material from the seawater-mixed concrete is significantly reduced. These observations confirm the hypothesis that ionic concentration gradients between the pore solution and surrounding environment causes leaching and negatively affect the compressive strengths in conventional concrete exposed to seawater. The leaching phenomena and the synergy between seawater and fly ash suggest that the long-term

performance of seawater-mixed concrete would be better compared with conventional concrete in seawater-submerged applications or marine environment, however, further testing is needed to conclusively demonstrate this.

Table 10 Water absorption and dry density

Mixture	Water Absorption (%)	Standard deviation (%)	Dry Density, kg/m^3 (lb/ft^3)	Standard deviation, kg/m^3 (lb/ft^3)
Mix A	3.46	0.14	2312 (144.3)	19 (1.1)
Mix B	2.79	0.08	2350 (146.7)	10 (0.6)

Conclusions

The following conclusions can be drawn from this study:

a) Comparable performance in terms of compressive strength was observed between conventional concrete and seawater-mixed concrete except in seawater at 60 °C (140 °F) in which seawater-mixed concrete performed better.

b) Strength differences between conventional concrete and seawater-mixed concrete may be explained by leaching effects.

c) A synergistic effect between seawater and fly ash seems to exist, which in part may explain the better performance of seawater-mixed concrete when exposed to seawater at 60 °C (140 °F).

d) Thermogravimetric analysis results confirmed that calcium hydroxide leached from the surface of the conventional concrete specimens after exposure to seawater at 60 °C (140 °F) after 24 months.

e) Electrical resistivity and formation factor were higher for seawater-mixed concrete compared to conventional concrete after exposure to seawater at 60 °C (140 °F) after 24 months.

f) Higher water absorption and a greater reduction in the density of conventional concrete compared to seawater-mixed concrete were observed after exposure to seawater at 60 °C (140 °F) after 24 months.

These results suggest that the long-term performance of seawater-mixed concrete could potentially be better compared with conventional concrete in seawater-submerged applications or marine environment.

CHAPTER 4

SHRINKAGE BEHAVIOR OF CEMENTITIOUS MATERIALS MIXED WITH SEAWATER

Background

Shrinkage behavior of cementitious materials mixed with seawater is investigated in this study. Shrinkage can cause cracking in the concrete, which increases the ingress of deleterious species into the concrete, which can lead to a reduction in the service life. The paste portion of the concrete tends to shrink due to consumption of water by hydration (autogenous shrinkage) or drying (drying shrinkage) [90, 91]. Water-to-cementitious materials ratio (w/cm), relative humidity, paste content, aggregate gradation, and supplementary cementitious materials (SCMs) are the main influencing factors of concrete shrinkage [90, 92].

To the best knowledge of the author, very little research has been performed on the shrinkage behavior of seawater-mixed concrete. Higher autogenous shrinkage for the seawater-mixed concrete compared with conventional concrete has been reported [93]. This has been attributed to refinement of the microstructure due to a higher degree of hydration in the seawater-mixed concrete. Some studies have shown that the use of seawater can enhance early age hydration and refine concrete microstructure [51, 63-65, 94]. Drying shrinkage increases significantly when the (admixed) chloride content in concrete increases, with a maximum increase of 200 μs when 1.2 % sodium chloride (by cement mass) was added [95]. The increasing drying shrinkage was attributed to microstructural refinement effect. Pore refinement can increase the surface tension in the gel and small capillary pores and therefore increase the drying shrinkage, which is caused

due to the capillary action upon the loss of water (pore fluid) from these pores [96]. A synergistic effect between seawater and fly ash in improving performance of seawater-mixed concrete in seawater and tidal-zone curing has been reported [97]. Other work has also shown synergy between SCMs and seawater resulting in increased pozzolanic reaction and pore refinement. Concrete containing slag has been shown to have a lower drying shrinkage when mixed with seawater as compared to concrete mixed with potable water, however, the authors did not explain their observations [58].

The objective of this study is to investigate the drying and autogenous shrinkage behavior of cementitious materials mixed with seawater. Cement mortar mixtures with two water-to-cementitious materials ratios (w/cm = 0.36 and 0.45), two binder compositions (namely, ordinary Portland cement (OPC) and OPC with 20 % fly ash replacement), and mixed with two types of water (tap water and seawater) were examined. Differences in shrinkage behavior are correlated to changes in mass, hydration, pore solution composition, porosity, and pore size distribution.

Materials and Methods

Materials

A type II cement meeting the requirements of ASTM C150/C150M-18, *Standard Specification for Portland Cement* [29], and a type F fly ash conforming to ASTM C618-17a, *Standard Specification for Coal Fly Ash and Raw or Calcined Natural Pozzolan for Use in Concrete* [30], were used in this study. Their oxide compositions and the phase composition of the cement are listed in **Table 11**. Tap water and seawater from Key Biscayne Bay (FL) were used as mixing water, with chemical composition (determined by

Inductively coupled plasma atomic emission spectroscopy [ICP-AES]) as shown in **Table 12**. Standard sand conforming to ASTM C778-17, *Standard Specification for Standard Sand* [98], passing No. 20 (850 μm) sieve with a specific gravity of 2.65 was used as the fine aggregate.

Table 11 Composition of the cement and fly ash.

Composition	**Mass (%)**	
	Type II cement	**Fly ash**
SiO_2	20.50	46.80
Al_2O_3	4.90	19.30
Fe_2O_3	3.90	18.99
CaO	64.40	5.50
MgO	0.90	0.90
SO_3	2.60	2.23
$Na_2O_{eq.}$	0.25	0.88
Loss on ignition	2.10	3.10
Bogue Phase Calculation*		
C_3S	60	-
C_2S	14	-
C_3A	7	-
C_4AF	12	-

*Note: According to cement chemistry notation, C is CaO, S is SiO_2, A is Al_2O_3, and F is Fe_2O_3.

Table 12 Chemical compositions of tap water and seawater used in concrete mixtures.

Ions	**Concentration (ppm)**	
	Tap Water	**Seawater**

Calcium	90	389
Chloride	44	18759
Iron	-	0.5
Potassium	6	329
Magnesium	6	1323
Sodium	26	9585
Sulfate	8	2489
Nitrate	1	0.1

Mortar Mixtures

Eight different mortar mixtures were examined, and their mixture proportions are shown in **Table 13**. Mixing was done in a mechanical mixer per ASTM C305-14 , *Standard Practice for Mechanical Mixing of Hydraulic Cement Pastes and Mortars of Plastic Consistency* [71]. Cementitious materials and sand were placed in the mixing bowl and dry mixed for 60 seconds. Then, the water was added and left to be absorbed for 15 seconds. The mixture was mixed at slow speed (140 ± 5 r/min) for 60 seconds and then at medium speed (285 ± 10 r/min) for 30 seconds. The mixer was paused for 90 seconds. During the first 30 seconds of this interval, the sides of the bowl were scraped, after which the mortar was left to stand in the bowl covered with the lid for 60 seconds. Finally, the mortar was mixed at medium speed (285 ± 10 r/min) for 60 seconds.

Table 13 Mortar mixture proportions.

Mixture ID	**Cement**	**Fly ash**	**Sand**	**Mixing water**		**w/cm**
				Seawater	**Tap water**	
OPC-TW-036	900	-	1800	-	324	0.36
OPC-FA-TW-036	720	180	1800	-	324	0.36

OPC-SW-036	900	-	1800	324	-	0.36
OPC-FA-SW-036	720	180	1800	324	-	0.36
OPC-TW-045	900	-	1800	-	405	0.45
OPC-FA-TW-045	720	180	1800		405	0.45
OPC-SW-045	900	-	1800	405	-	0.45
OPC-FA-SW-045	720	180	1800	405	-	0.45

Autogenous Shrinkage

Autogenous shrinkage was measured for each mortar mixture following ASTM C1698-09(2014), *Standard Test Method for Autogenous Strain of Cement Paste and Mortar* [99]. Freshly mixed mortar was poured into a corrugated polyethylene mold, closed at one end with an end plug and inserted into a support tube positioned vertically on a vibrating table. Molds were filled in four equal layers compacted with tamping rod, after which the top end plug was mounted such that it was in contact with the mortar. Three replicate specimens were cast for each mortar mixture. The specimens were stored horizontally on a smooth surface at an ambient temperature at 23 ± 2 ° C. The length change measurements were started from the time of final setting for a period of 65 days using a dilatometer with a digital length gauge at intervals of three hours during the first day, twice a day during the first month, and once a day afterwards. The final setting time of the corresponding cement pastes was also measured by Vicat needle per ASTM C191-18, *Standard Test Methods for Time of Setting of Hydraulic Cement by Vicat Needle* [70]. The paste samples were mixed using mechanical mixer per ASTM C305-14, *Standard Practice for Mechanical Mixing of Hydraulic Cement Pastes and Mortars of Plastic Consistency* [71]. Mixing water was placed in the mixing bowl to which cement was added and left to absorb water for 30 seconds. Then, the mixture was mixed at slow speed (140 ± 5 r/min) for 30 seconds. The

mixer was paused for 15 seconds in order to scrape the sides of the bowl, after which the mixture was mixed for 60 seconds at medium speed (285 ± 10 r/min). The mass change was monitored to ensure that there was no moisture loss during the test.

Drying Shrinkage

Drying shrinkage of each mortar mixture was measured per ASTM C596-09(2017), *Standard Test Method for Drying Shrinkage of Mortar Containing Hydraulic Cement* [100]. Three prisms with dimensions of 25 x 25 x 285 mm were cast from each mortar mixtures. Molds were filled in two equal layers and compacted using vibrating table. Specimens were moist cured in the mold at 100% relative humidity and temperature of 23 ± 2 °C for 24 hours, then removed from the molds and cured in a saturated lime solution for 48 hours. For curing the seawater-mixed specimens, saturated lime solution was made with seawater instead of tap water in order to minimize the leaching of alkalis and calcium hydroxide [97]. At the age of 72 hours, the specimens were removed from the storage solution, wiped with damp cloth, measured using length comparator and moved to a desiccator with 50 ± 4 % relative humidity and temperature of 23 ± 2 °C. The length change measurements were performed at intervals of twice a day during the first month, and once a day afterwards for a period of 65 days. The mass change of the drying shrinkage specimens was monitored over the duration of the test.

Isothermal Calorimetry

Paste samples using the same mixture design as the mortars in **Table 13** were mixed manually for isothermal calorimetry testing. For each mixture, 40 g of material was mixed

in a plastic container using a spatula for 4 minutes. Approximately 7 grams of paste was poured into a glass ampoule, which was gently tamped to consolidate and sealed with a lid to ensure there is not any moisture evaporation during the experiment. The specimens were then placed in an isothermal calorimeter (TAM Air, TA Instruments), which was preconditioned at 23 ± 0.05 °C. The heat flow and the cumulative heat release were measured for a period of 60 hours in order to quantify potential early age differences in the hydration kinetics induced by seawater and fly ash.

Thermogravimetric Analysis (TGA)

Thermogravimetric analysis (TGA) was performed on the paste samples, which were tested in the isothermal calorimetry at an age of 21 days to determine potential later age changes in hydrate assemblage induced by seawater and fly ash. Paste samples were extracted from the ampoules and gently crushed using a mortar and pestle. The TGA (TGA 55, TA instruments) was performed in an inert nitrogen atmosphere by increasing the temperature at the rate of 10 °C per minute from 23 °C to 1000 °C. The tangent method was used to quantify the amount of calcium hydroxide present in the sample [78].

While shrinkage measurements, isothermal calorimetry, and TGA were performed on all mixtures, a rather strong effect of the seawater on the drying shrinkage at w/cm 0.45 was observed. In order to explain this effect, additional testing was performed on mixtures with seawater at w/cm 0.45.

Water Absorption, Density, and Volume of Voids

Water absorption, density, and voids volume measurements were conducted on the

mortar prisms with w/cm 0.45 after the drying shrinkage test was completed. Three slices with a thickness of 5 mm were cut from the cross section of these prisms and immersed in simulated pore solution at 23 ± 2 °C. Simulated pore solution was prepared with the following composition: 0.23 M NaOH, 0.56 M KOH, and 0.05 M $Ca(OH)_2$ [101] and was used in order to minimize the leaching of calcium hydroxide and alkalis into the solution [82]. Specimens were removed from the storage solution after 72 hours, wiped with a cloth to achieve saturated surface dry conditions, and weighed to determine the saturated mass. Immersed apparent mass was also measured while suspending the specimens by a wire in the distilled water. Then, saturated specimens were dried in an oven at 55 °C for 24 hours to find the oven-dry mass. The following equations were used to calculate the density, water absorption, and volume of permeable pore space (voids):

$$Water\ absorption\ (\%) = \frac{Saturated\ mass - Oven\ dry\ mass}{Oven\ dry\ mass} \times 100 \quad (3)$$

$$Dry\ density\ \left(\frac{kg}{m^3}\right) = \frac{Oven\ dry\ mass}{Sauturated\ mass - Apparent\ mass} \times Density\ of\ water \quad (4)$$

$$Apparent\ density\ \left(\frac{kg}{m^3}\right) = \frac{Oven\ dry\ mass}{Oven\ dry\ mass - Apparent\ mass} \times Density\ of\ water \quad (5)$$

$$Volume\ of\ voids\ (\%) = \frac{Apparent\ density - Dry\ density}{Apparent\ density} \times 100 \quad (6)$$

Results and Discussion

Autogenous Shrinkage

Fig. 20 shows the evolution of autogenous shrinkage of the mortar mixtures with w/cm 0.36. Representative error shown in **Fig. 20** is the average of the error values obtained for all data points and the error bars are one standard deviation of the average on each side for

this and subsequent figures. The use of seawater increased the ultimate autogenous shrinkage from 213 μs in the OPC mixture with tap water to 387 μs in the mixture with seawater; corresponding values for the fly ash mixture were 230 μs and 449 μs. Seawater prominently increases the autogenous shrinkage at early ages. As an example, at 10 days, the use of seawater increases the autogenous shrinkage from 180 μs to 347 μs in OPC mixtures; subsequent changes in the shrinkage are minor for both mixtures. This is likely caused by the early age acceleration in hydration known to be caused by seawater [63-65]. On the other hand, the use of fly ash decreases early age shrinkage, presumably due to dilution effects [102], however, it increases autogenous shrinkage at later ages, shown by the greater slope in the shrinkage in mixtures with fly ash. In mixtures without fly ash, the autogenous shrinkage increases only slightly after 10 days, however, this increase is more prominent in mixtures with fly ash. The largest value of shrinkage (449 μs) is observed in the mixture with seawater and fly ash. This could be explained by a kind of "pessimum" behavior – an increase that is equal to the sum of the early age increase due to seawater and the later age increase due to the fly ash.

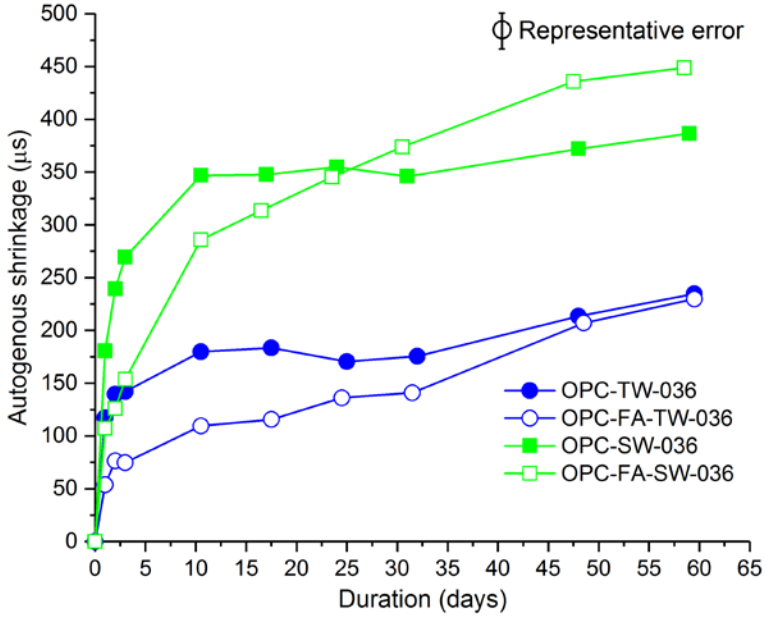

Fig. 20 Autogenous shrinkage of the mortar mixtures with w/cm 0.36.

The autogenous shrinkage values of the mortar mixtures with w/cm 0.45 are shown in **Fig. 21**. The autogenous shrinkage strains were generally lower compared with the mortar mixtures mixed with w/cm 0.36 (**Fig. 20**), due to the higher w/cm [90]. The general trends in autogenous shrinkage at w/cm 0.45 are similar to w/cm 0.36. The use of seawater resulted in increasing autogenous shrinkage. The ultimate shrinkage increased from 149 µs to 314 µs for the OPC mixtures and from 175 µs to 287 µs for the fly ash mixtures due to the use of seawater. As with w/cm 0.36, seawater increases the autogenous shrinkage at early ages and fly ash increases the rate of autogenous shrinkage at later ages. However, unlike the case with w/cm 0.36, the largest value of shrinkage (314 µs) is observed in the OPC mixture with seawater. This may be because of greater availability of water in a sealed system for hydration and pozzolanic reaction at w/cm 0.45. These results are generally

consistent with literature which has shown that seawater results in an increase in early age autogenous shrinkage [93].

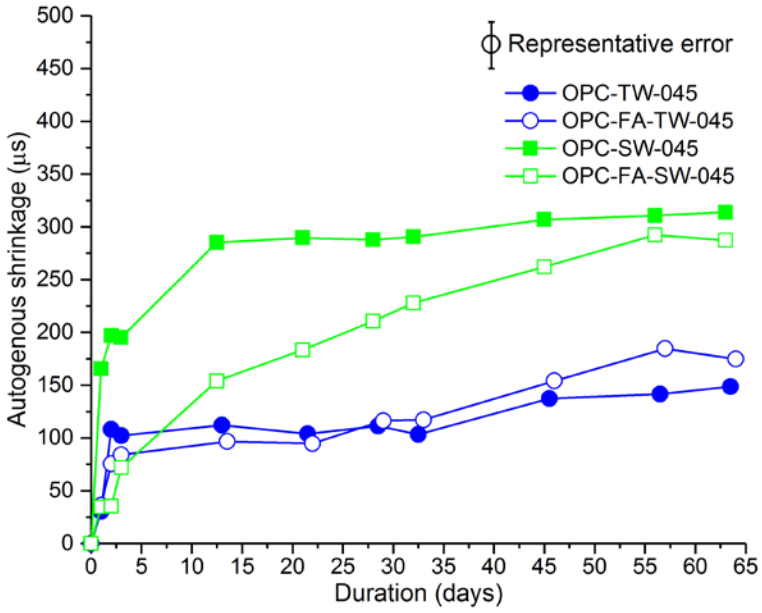

Fig. 21 Autogenous shrinkage of the mortar mixtures with w/cm 0.45.

Drying Shrinkage

The drying shrinkage strains of the mortar mixtures with w/cm 0.36 are shown in **Fig. 22**. In general, the drying shrinkage behavior of these mixtures is similar, with ultimate values ranging from 543 µs to 663 µs. While shrinkage values are extremely similar before 40 days, some divergence is observed between 40 and 60 days. The ultimate shrinkage increased from 562 µs to 617 µs for the OPC mixtures and from 543 µs to 663 µs for the fly ash mixtures due to the use of seawater. Unlike the autogenous shrinkage, which is more prominent at early ages, the drying shrinkage continues to increase, almost linearly, through the duration of the test. The largest value of shrinkage (663 µs) is observed in the

mixture with seawater and fly ash. This could potentially be explained by a synergistic effect of seawater and fly ash, which leads to a finer capillary pore structure [63, 66], although it is not clear why such an effect would be seen only after 40 days.

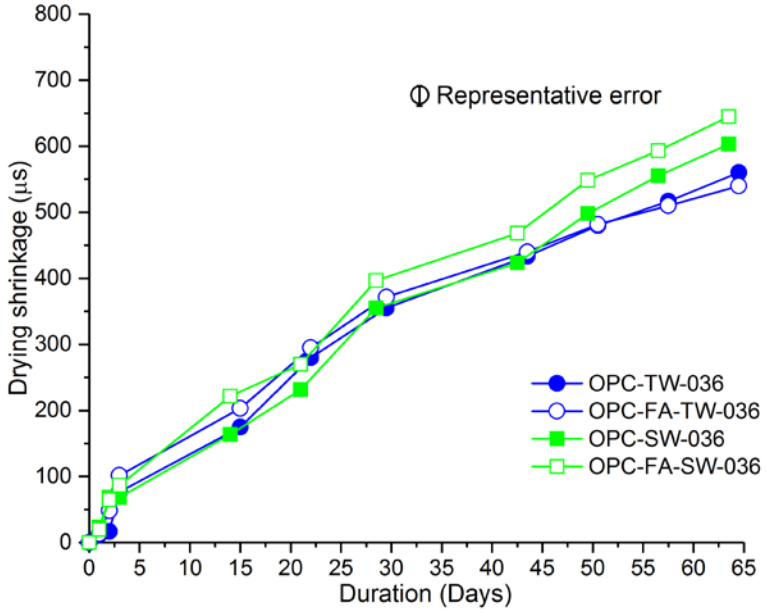

Fig. 22 Drying shrinkage of the mortar mixtures with w/cm 0.36.

Fig. 23 shows the drying shrinkage strains of the mortar mixtures with w/cm 0.45. The ultimate drying shrinkage values are much higher in this case compared to w/cm 0.36, with recorded shrinkage in the range of 738 µs to 1325 µs. The ultimate shrinkage increased from 838 µs to 980 µs for the OPC mixtures and from 738 µs to 1325 µs for the fly ash mixtures due to the use of seawater. Fly ash seems to decrease the shrinkage in mixtures with tap water, however, in mixtures with seawater, a very strong increase in shrinkage is observed, and the mixture with fly ash and seawater shows by far the highest drying shrinkage of all the mixtures (1325 µs). This increase in the mixture with fly ash and

seawater is apparent even at 10 days. This results may potentially be explained by a synergistic effect of seawater and fly ash which leads to a finer capillary pore structure [63, 66], although it is not clear why this effect would manifest so strongly and so differently from the one seen at w/cm 0.36.

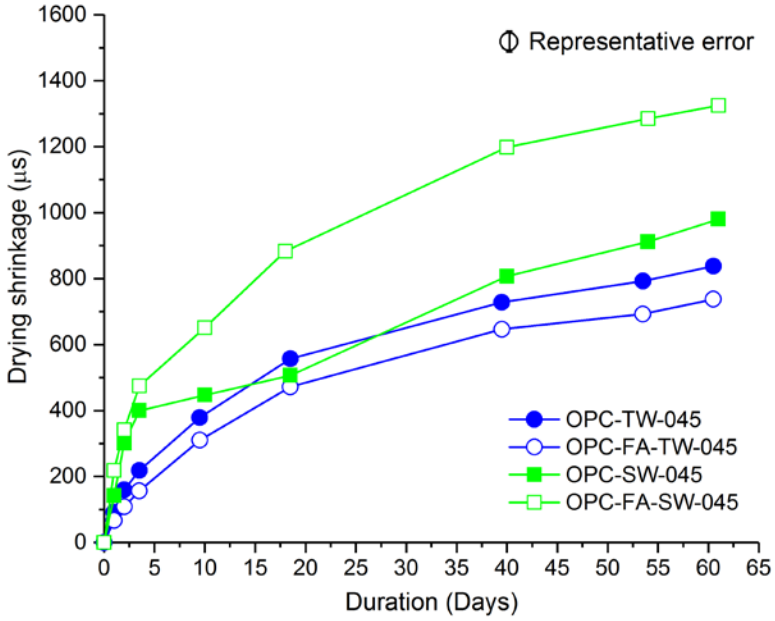

Fig. 23 Drying shrinkage of the mortar mixtures with w/cm 0.45.

In order to better understand the effect of seawater on the drying shrinkage, mass loss was measured for the mortar mixtures. **Fig. 24** shows the mass loss of the mortar mixtures with w/cm 0.36 during the 60-day period of drying. The use of seawater decreases the ultimate mass loss from 1.28 % to 0.25 % for the OPC mixture, however, no significant change was observed for the mixture with fly ash. Fly ash increased the mass loss from 1.28 % to 1.86 % when mixed with fresh water and from 0.25 % to 1.73 % for seawater-mixed mortar. The seawater-mixed mortar with fly ash shows a sharp mass loss in the first

5 days for unclear reasons.

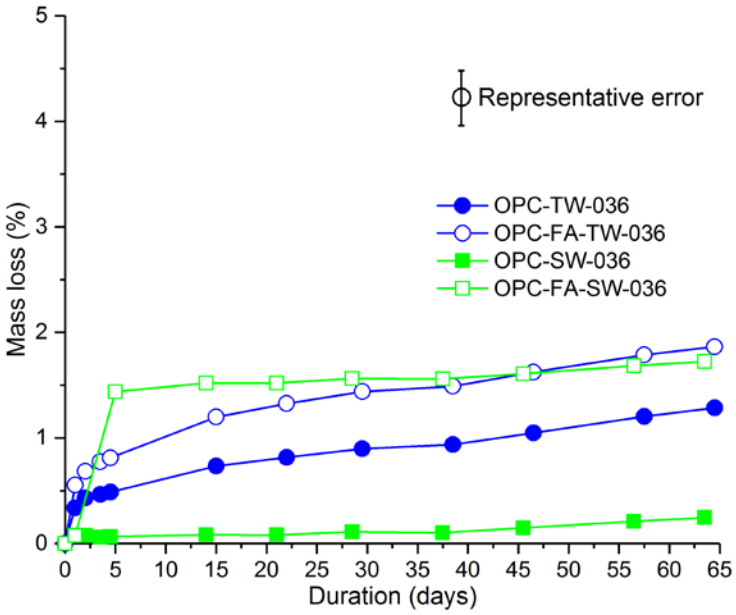

Fig. 24 Mass loss of the mortar mixtures with w/cm 0.36.

The mass loss of the mortar mixtures with w/cm 0.45 is shown in **Fig. 25**. The mass loss values are higher compared to 0.36 w/cm and ranged from 0.59 % to 3.45 %. The use of seawater decreases the mass loss from 2.49 % to 0.59 % for the OPC mixture and from 3.45 % to 2.08 % for the fly ash mixture. Fly ash increases the mass loss from 2.49 % to 3.45 % when mixed with fresh water and from 0.59 % to 2.08 % for seawater-mixed mortar. These differences may be explained by changes in microstructural evolution as seawater leads to a higher degree of hydration and a denser microstructure [51, 63-65], whereas fly ash could result in an increase in the total porosity [103, 104].

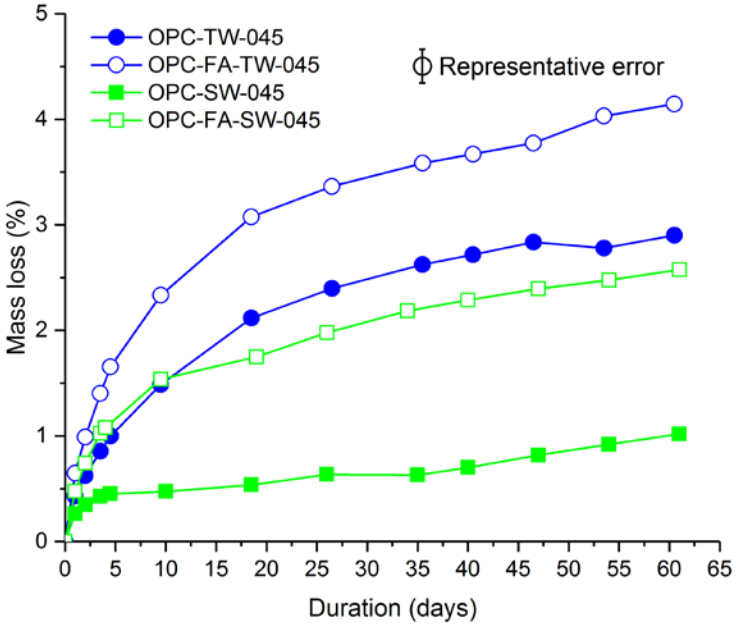

Fig. 25 Mass loss of the mortar mixtures with w/cm 0.45.

Isothermal Calorimetry and Thermogravimetric Analysis

The heat flow and the cumulative heat release data for 60 hours are shown in **Fig. 26** and **Fig. 27**, respectively. Seawater causes an accelerating effect, as expected [63]- the silicate peaks occur at an earlier age and the cumulative heat release is higher in mixtures with seawater than with tap water. Fly ash causes a reduction in the early age cumulative heat release. These observations explain early age trends in autogenous shrinkage shown earlier. While some differences in behavior based on w/cm are observed, a strong synergistic effect of the fly ash and seawater cannot be confirmed at early ages from isothermal calorimetry.

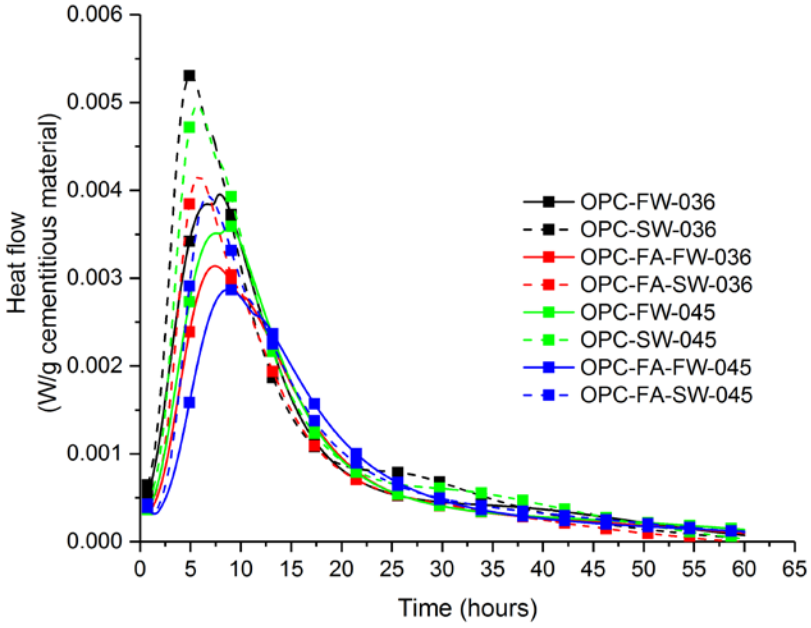

Fig. 26 Heat flow for the tested paste mixtures.

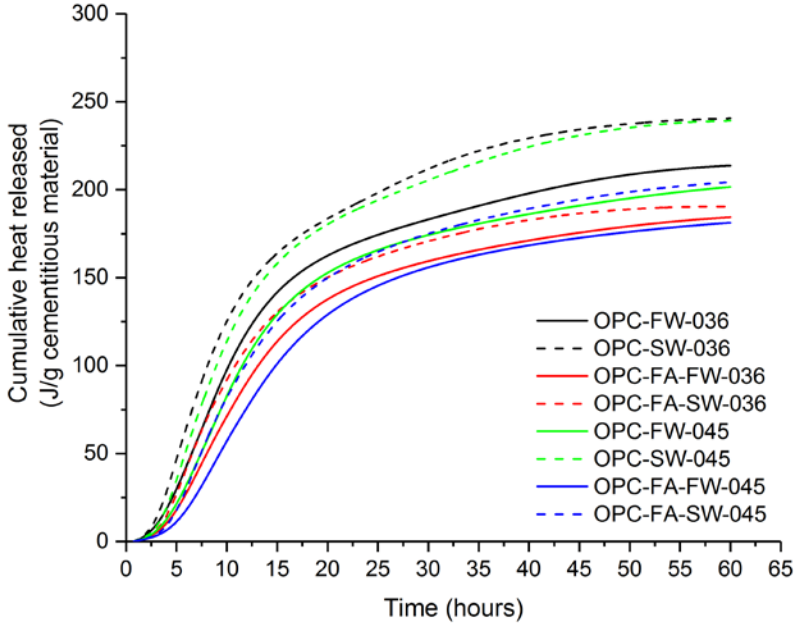

Fig. 27 Cumulative heat release for the tested paste mixtures.

The calcium hydroxide content of the mixtures at 21 days is measured using TGA and the results are presented in **Table 14**. At this age, fly ash mixtures have a lower calcium hydroxide content, but mixtures with OPC have very similar calcium hydroxide content. No obvious effect of the seawater is observed at this age. These results suggest that the accelerating effect of seawater is minimal at this age, in agreement with literature [63]. The amount of free water present in the mixtures was computed using the loss of mass from 23 °C to 105 °C from the thermograph and normalizing it to the mass at 23 °C. The only significant difference in the mixtures in the free water content is the free water loss in the mixture with fly ash and seawater with w/cm 0.45, which is the highest (15.87 %). However, such measures may be complicated by water loss from aluminate phases, in addition, it is unclear if this difference is statistically significant.

Table 14 Calcium hydroxide content and free water loss (both expressed as a % of the original paste mass).

Mixture ID	Calcium hydroxide content, %	Free water loss, %
OPC-TW-036	12.86	12.27
OPC-FA-TW-036	10.92	12.51
OPC-SW-036	12.73	13.10
OPC-FA-SW-036	10.94	12.97
OPC-TW-045	14.44	14.66
OPC-FA-TW-045	11.40	14.39
OPC-SW-045	14.61	15.04
OPC-FA-SW-045	11.94	15.87

Water Absorption, Density, and Voids Volume

Water absorption, density, and voids volume of the mortar mixtures with w/cm 0.45 after 60 days of drying is shown in **Table 15**. These results are in agreement with the mass loss measurements. Seawater increases the density and decreases the volume of the voids and water absorption. This reduction in the amount of voids likely leads to a lower mass loss. Similar trends have been suggested in literature [65, 93, 99]. Fly ash increases the volume of the voids and the water absorption, which could result in higher mass loss. The higher autogenous and drying shrinkage values observed in mixtures with fly ash and seawater cannot be explained directly using density and porosity measurements as these do not measure pore size.

Table 15 Water absorption, dry density, and voids volume (standard deviation values are shown in the parenthesis).

Mixture ID	Water absorption, %	Dry density, kg/m^3	Volume of voids, %
OPC-TW-045	6.78 (0.22)	2169 (8.10)	14.71 (0.44)
OPC-FA-TW-045	7.34 (0.06)	2174 (6.86)	15.95 (0.10)
OPC-SW-045	6.06 (0.18)	2228 (17.39)	13.49 (0.31)
OPC-FA-SW-045	6.62 (0.07)	2212 (4.41)	14.65 (0.15)

While seawater may also enhance the hydration of the fly ash, such an effect is not seen in TGA results at 21 days (although longer term enhancement cannot be ruled out). Seawater and fly ash both change pore solution ionic concentrations, however, the ionic strength of seawater-mixed cement paste is known to slightly higher than that of seawater-mixed cement paste with fly ash [63], therefore, these observations cannot be explained by

pore solution composition either.

Therefore, the two reasons which may explain the high values of drying shrinkage observed in the seawater-mixed mortar with fly ash at w/cm 0.45 are:

a) Pore refinement – This is known to be caused due to fly ash [103], but seawater also has been shown to result in pore refinement [64, 65, 94]. Therefore, the use of fly ash and seawater together may result in a shift in the pore sizes towards even finer pores.

b) Drying rate – It appears that the use of seawater and the pore refinement results in a reduction of the drying rate of the mortar (**Fig. 6**). It is possible that the water (pore fluid) does not leave the sample, but instead moves inside the mortar microstructure, causing a consolidation of the different layers of C-S-H gel, resulting in increased shrinkage, which is not necessarily reflected as a mass loss [105].

Conclusions

The following conclusions can be drawn from this study:

a) The use of seawater as mixing water increases the autogenous shrinkage. An acceleration of the cement hydration at early ages due to the seawater is identified as the cause of the increase in autogenous shrinkage in mixtures with seawater.

b) Fly ash increases the autogenous shrinkage at later ages. The mixture with seawater and fly ash showed the highest autogenous shrinkage which could be due to the combined early age increase due to seawater and later age increase due to the fly ash.

c) The use of seawater and fly ash do not have a large impact on the drying shrinkage in mortar mixtures with w/cm 0.36.

d) Seawater increases the drying shrinkage and the use of seawater and fly ash together drastically increase the drying shrinkage in mortar mixtures with w/cm 0.45. The increase is likely due to a finer pore size distribution and internal water movement.
e) The use of fly ash in seawater-mixed concrete could be problematic in applications where drying shrinkage may be a concern. However, fly ash increases the workability, therefore, w/cm could be reduced which counteract seawater effect.

Seawater increased the shrinkage, therefore, care should be taken when using seawater-mixed concrete in the applications where shrinkage might be an issue. However, most of the applications of the seawater-mixed concrete are in the coastal regions in which shrinkage may not be a concern due to the high relative humidity. In addition, the seawater effect can be controlled by controlling w/cm as the main factor influencing shrinkage.

CHAPTER 5

CONCLUSIONS

The main objective of this dissertation was to have a better understanding of the fundamental behavior of the seawater-mixed concrete and embedded GFRP bars. To this end, durability of GFRP bars in seawater-mixed concrete (*Study 1*), compressive strength development of seawater-mixed concrete in different curing regimes (*Study 2*) and shrinkage behavior of seawater-mixed concrete were studied (*Study 3*).

Study 1 investigated the effect of seawater used as mixing water in concrete on the long-term properties of GFRP bars. This was one of the few research efforts that examined the durability of GFRP reinforcements in seawater-mixed concrete. Although the durability of GFRP bars have been studied in detail by many researchers, the effect of certain ions of seawater (i.e., chloride, sodium, potassium, etc.) on the durability of GFRP bar and its degradation mechanism was still unclear. The durability of GFRP bars embedded in seawater-mixed concrete was studied in terms of residual mechanical properties (i.e. tensile strength, horizontal and transverse shear strength, and GFRP-concrete bond strength) after immersion in seawater at 60 °C for a period of 24 months. SEM was used to identify degradation mechanisms. The results presented in this study are in the general agreement with literature, however, due to the high variance in the GFRP materials, exposure conditions, exposure temperature, and quality of surrounding concrete, direct comparison between the collected results and literature was not possible. It was concluded that using seawater as the mixing water has no effect on the durability of GFRP bars. The following conclusions can be drawn from this study:

a) Extracted GFRP bars from the conventional and seawater-mixed concrete showed comparable performance indicating that using seawater as mixing water has no significant effect on the durability of GFRP bars.
b) Tensile and shear strength properties showed a moderate reduction after 24-month immersion in seawater at 60 °C.
c) The bond strength showed the highest degradation for both concrete mixtures.
d) Micrographs showed a large number of defects (voids) near the edge of the bars, which may have been formed during manufacturing. These defects (voids) provide a pathway for alkalis, which can cause local damage in the forms of fiber disintegration and de-bonding between fibers and resin matrix. More fibers are affected over time, leading to circumferential cracks near the edge. This leads to a degradation of the edge (surface), which explains the large reduction in the bond strength, compared to other mechanical properties.

Unless industry develops consensus standards on composition, manufacturing and type of surface enhancement for bond with concrete, each commercially available GFRP bar system will have to be thoroughly tested in order to assess its performance and long-term durability. Generic statements about "all" bars are not possible. As a result of research studies like the one presented here, GFRP manufacturers have been able to detect the defects and improve their products. It should be noted that the bars tested in this study are categorized as the first generation of the GFRP bars. As manufacturing techniques have improved over time, the quality and durability of bars also improved. Research has shown that the second generation of the GFRP bars are significantly more durable in terms of mechanical properties when exposed to the same accelerated aging [49].

Study 2 reported the results of an investigation on the effect of different environments (curing regimes) on the compressive strength development of seawater-mixed concrete. Despite several studies on the long-term performance of concrete mixed with seawater, little research has been performed on a direct comparison of conventional concrete and seawater-mixed concrete in various environments. Concrete cylinders were cast and exposed to subtropical environment (outdoor exposure), tidal zone (wet-dry cycles), moist curing (in a fog room), and seawater at 60 °C (140 °F) (submerged in a tank). Thermogravimetric Analysis (TGA), Energy-dispersive X-ray spectroscopy (EDX), and electrical resistivity measurements were performed at the end of 24 months on specimens exposed to seawater at 60 °C (140 °F). It was shown that seawater-mixed concrete performs better in terms of strength when exposed to marine environment. This is due to the leaching effect, which was confirmed by additional testing using TGA, EDX, and electrical resistivity measurements. The following conclusions can be drawn from this study:

a) Comparable performance in terms of compressive strength was observed between conventional concrete and seawater-mixed concrete except in seawater at 60 °C (140 °F) in which seawater-mixed concrete performed better.
b) Strength differences between conventional concrete and seawater-mixed concrete may be explained by leaching effects.
c) A synergistic effect between seawater and fly ash seems to exist, which in part may explain the better performance of seawater-mixed concrete when exposed to seawater at 60 °C (140 °F).

d) Thermogravimetric analysis results confirmed that calcium hydroxide leached from the surface of the conventional concrete specimens after exposure to seawater at 60 °C (140 °F) after 24 months.
e) Electrical resistivity and formation factor were higher for seawater-mixed concrete compared to conventional concrete after exposure to seawater at 60 °C (140 °F) after 24 months.
f) Higher water absorption and a greater reduction in the density of conventional concrete compared to seawater-mixed concrete were observed after exposure to seawater at 60 °C (140 °F) after 24 months.

These results suggest that the long-term performance of seawater-mixed concrete could potentially be better compared with conventional concrete in seawater-submerged applications or marine environment.

Study 3 examined the autogenous and drying shrinkage behavior of cementitious materials mixed with seawater. To the best knowledge of the author, very little research has been performed on the shrinkage behavior of seawater-mixed concrete. Shrinkage was of an interest as one of the durability aspects since it causes cracking which provides a pathway for deleterious species into the concrete. Cement mortar mixtures were prepared with two water-to-cementitious materials ratios (w/cm = 0.36 and 0.45), two binder compositions (namely, ordinary Portland cement (OPC) and OPC with 20 % fly ash replacement), and two types of water (tap water and seawater). The autogenous and drying shrinkage behavior of these mixtures are examined using ASTM standard test methods for 60 days. Differences in shrinkage behavior are correlated to changes in mass, hydration, pore solution composition, porosity, and pore size distribution. Seawater increased the

shrinkage by refining the pore structure. When seawater mixed with fly ash, this refinement was amplified and affected shrinkage significantly. However, further testing is needed to conclusively demonstrate this. The following conclusions can be drawn from this study:

a) The use of seawater as mixing water increases the autogenous shrinkage. An acceleration of the cement hydration at early ages due to the seawater is identified as the cause of the increase in autogenous shrinkage in mixtures with seawater.
b) Fly ash increases the autogenous shrinkage at later ages. The mixture with seawater and fly ash showed the highest autogenous shrinkage which could be due to the combined early age increase due to seawater and later age increase due to the fly ash.
c) The use of seawater and fly ash do not have a large impact on the drying shrinkage in mortar mixtures with w/cm 0.36.
d) Seawater increases the drying shrinkage and the use of seawater and fly ash together drastically increase the drying shrinkage in mortar mixtures with w/cm 0.45. The increase is likely due to a finer pore size distribution and internal water movement.
e) The use of fly ash in seawater-mixed concrete could be problematic in applications where drying shrinkage may be a concern. However, fly ash increases the workability, therefore, w/cm could be reduced which counteract seawater effect.

Seawater increased the shrinkage, therefore, care should be taken when using seawater-mixed concrete in the applications where shrinkage might be an issue. However, most of the applications of the seawater-mixed concrete are in the coastal regions in which shrinkage may not be a concern due to the high relative humidity. In addition, the seawater effect can be controlled by controlling w/cm as the main factor influencing shrinkage.

Future Research

In order to reach the full potential of such a technology, further research and more experimental works are needed. The results presented in this study are mainly collected by aging the specimens in the accelerated manner using elevated temperature as the accelerating factor, however, the actual long-term performance needs to be studied.

The effect of seawater on the long-term durability of GFRP bar and its degradation mechanisms needs to be examined in the field by monitoring the performance of real size structures built with seawater-mixed concrete and reinforced with GFRP bars. Demo projects like Halls River Bridge in Homosassa, FL, in which seawater-mixed concrete reinforced with composite bars such as GFRP was used to build the bulkhead cap, will allow us to monitor the performance of this technology in service. As mentioned before, GFRP bars tested in this study are categorized as the first generation. Testing the second generation of the GFRP bars using the same experimental program can provide us with useful insights for assessing the long-term durability of GFRP reinforcement in seawater-mixed concrete.

The same scenario of accelerated aging is applicable to the compressive strength development of the seawater-mixed concrete. Leaching effect was shown for the specimens exposed to seawater at 60 °C, however, the leaching extent in other curing regimes such as tidal zone could also be of an interest. The change of this leaching with time and its effect on the long-term compressive strength of seawater-mixed concrete can be further investigated. Fly ash was used in this study, however, the effect of other SCMs such as slag could be interesting.

It was shown that seawater increases the shrinkage and when mixed with fly ash the seawater effect was amplified. The effect of other SCMs on the shrinkage behavior of seawater-mixed concrete needs further investigation. Furthermore, the mitigation techniques such as shrinkage reducing admixtures, lightweight aggregate, calcium sulfoaluminate (CSA), and super absorbent polymer (SAP) could be of an interest. Shrinkage was the only durability aspect of seawater-mixed concrete studied here, therefore, assessing durability in terms of sulfate attack, alkali silica reaction, and freeze-thaw could pave the way for implementing this technology.

BIBLIOGRAPHY

1. WHO, W.H.O., *Global water supply and sanitation assessment 2000 report*. 2000, World Health Organization (WHO) and the United Nations Children's Fund (UNICEF): Geneva.

2. SBCI, S.B.C.I., *Buildings and climate change: Summary for decision makers*. 2009, UN Environment Programme: Paris, France.

3. Gleick, P.H., *Water in crisis: A guide to the world's fresh water resources*. 1993, New York, NY: Oxford University Press.

4. Chung, E. *Most groundwater is effectively a non-renewable resource, study finds*. CBC News, 2015.

5. Scrivener, K.L., V.M. John, and E.M. Gartner, *Eco-efficient cements: Potential economically viable solutions for a low-CO_2 cement-based materials industry.* Cement and Concrete Research, 2018.

6. Hadley, H., *Letter to editor*, in *Engineering News-Record*. 1935. p. 716-717.

7. ACI, *Job problems and practice*. 1940, American Concrete Institute. p. 313-314.

8. Ghorab, H., M. Hilal, and E. Kishar, *Effect of mixing and curing waters on the behaviour of cement pastes and concrete part 1: Microstructure of cement pastes.* Cement and Concrete Research, 1989. 19(6): p. 868-878.

9. Nanni, A., A. De Luca, and H.J. Zadeh, *FRP reinforced concrete structures–theory, design and practice*. 2014, Boca Raton, FL: CRC Press.

10. Hao, Q., et al., *Bond strength of glass fiber reinforced polymer ribbed rebars in normal strength concrete.* Construction and Building Materials, 2009. 23(2): p. 865-871.

11. Zhou, J., X. Chen, and S. Chen, *Effect of different environments on bond strength of glass fiber-reinforced polymer and steel reinforcing bars.* KSCE Journal of Civil Engineering, 2012. 16(6): p. 994-1002.

12. Bank, L.C., M. Puterman, and A. Katz, *The effect of material degradation on bond properties of fiber reinforced plastic reinforcing bars in concrete.* ACI Materials Journal, 1998. 95(3): p. 232-243.

13. Chen, Y., et al., *Accelerated aging tests for evaluations of durability performance of FRP reinforcing bars for concrete structures.* Composite Structures, 2007. 78(1): p. 101-111.

14. Abbasi, A. and P.J. Hogg, *Temperature and environmental effects on glass fibre rebar: modulus, strength and interfacial bond strength with concrete.* Composites Part B: Engineering, 2005. 36(5): p. 394-404.

15. Robert, M. and B. Benmokrane, *Effect of aging on bond of GFRP bars embedded in concrete.* Cement and Concrete Composites, 2010. 32(6): p. 461-467.

16. Bank, L., M. Puterman, and A. Katz, *The effect of material degradation on bond properties of FRP reinforcing bars in concrete.* ACI Materials Journal, 1998. 95: p. 232-243.

17. Micelli, F. and A. Nanni, *Durability of FRP rods for concrete structures.* Construction and Building Materials, 2004. 18(7): p. 491-503.

18. Gooranorimi, O. and A. Nanni, *GFRP reinforcement in concrete after 15 years of service.* Journal of Composites for Construction, 2017. 21(5): p. 04017024.

19. Mufti, A.A., et al., *Durability of GFRP composite rods.* Concrete International, 2007. 29(02).

20. Porter, M.L., Mehus, J., Young, K. A., O'Neil, E. F., and Barnes, B. A., *Aging for fiber reinforcement in concrete*, in *3rd Int. Symp. on Non-Metallic (FRP) Reinforcement for Concrete Structures*. 1997: Sapporo, Japan. p. 59-66.

21. Katsuki, F., *Prediction of deterioration of FRP rods due to alkali attack*, in *Second International RILEM Symposium: Non-Metallic (FRP) Reinforcement for Concrete Structures*. 1995, CRC Press. p. 82.

22. Murphy, K., S. Zhang, and V. Karbhari, *Effect of concrete based alkaline solutions on short term response of composites.* Society for the Advancement of Material and Process Engineering, Evolving and Revolutionary Technologies for the New Millenium, 1999. 44: p. 2222-2230.

23. Robert, M. and B. Benmokrane, *Combined effects of saline solution and moist concrete on long-term durability of GFRP reinforcing bars.* Construction and Building Materials, 2013. 38: p. 274-284.

24. El-Maaddawy, T., A. Al-Saidy, and A. Al-Sallamin, *Residual strength of glass fiber reinforced polymer bars in seawater-contaminated concrete*, in *International workshop on seawater sea-sand concrete (SSC) structures reinforced with FRP composites*. 2016: Hong Kong, China.

25. Byars, E.A., et al., *Durability of FRP in concrete - Deterioration mechanisms.* International Journal of Materials and Product Technology, 2003. 19: p. 28-39.

26. Robert, M., P. Cousin, and B. Benmokrane, *Durability of GFRP reinforcing bars embedded in moist concrete.* Journal of Composites for Construction, 2009. 13(2): p. 66-73.

27. Bank, L.C., et al., *A model specification for FRP composites for civil engineering structures.* Construction and Building Materials, 2003. 17(6–7): p. 405-437.

28. Ruiz Emparanza, A., R. Kampmann, and F.J. De Caso y Basalo, *State-of-the-practice of FRP rebar global manufacturing*, in *The Composites and Advanced Materials Expo (CAMX 2017)*. 2017: Orlando, Florida.

29. ASTM, *ASTM C150/C150M-18 standard specification for portland cement* 2018, ASTM International: West Conshohocken, PA.

30. ASTM, *ASTM C618-17a standard specification for coal fly ash and raw or calcined natural pozzolan for use in concrete*. 2017, ASTM International: West Conshohocken, PA.

31. Khatibmasjedi, S., F.J. De Caso y Basalo, and A. Nanni, *SEACON: Redefining sustainable concrete*, in *Fourth International Conference on Sustainable Construction Materials and Technologies*. 2016: Las Vegas, NV.

32. ICC-ES, *AC-454: Acceptance criteria for fiber-reinforced polymers (FRP) bars for internal reinforcement of concrete members*. 2015, International Code Council-Evaluation Services: Whittier, CA.

33. ASTM, *ASTM D792-13 standard test methods for density and specific gravity (relative density) of plastics by displacement*. 2013, ASTM International: West Conshohocken, PA.

34. ASTM, *ASTM D2584-11 standard test method for ignition loss of cured reinforced resins*. 2011, ASTM International: West Conshohocken, PA.

35. ASTM, *ASTM D570-98(2010)e1 standard test method for water absorption of plastics*. 2010, ASTM International: West Conshohocken, PA.

36. ASTM, *ASTM D7205/D7205M-06(2016) standard test method for tensile properties of fiber reinforced polymer matrix composite bars*. 2016, ASTM International: West Conshohocken, PA.

37. ASTM, *ASTM D4475-02(2016) standard test method for apparent horizontal shear strength of pultruded reinforced plastic rods by the short-beam method*. 2016, ASTM International: West Conshohocken, PA.

38. ASTM, *ASTM D7617/D7617M-11(2017) standard test method for transverse shear strength of fiber-reinforced polymer matrix composite bars*. 2017, ASTM International: West Conshohocken, PA.

39. Khatibmasjedi, M. and A. Nanni, *Durability of GFRP reinforcement in SEACON*, in *The Fifth International Conference on Durability of Fiber Reinforced Polymer (FRP) Composites for Construction and Rehabilitation of Structures (CDCC 2017)*. 2017: Sherbrooke, Quebec, CANADA.

40. ASTM, *ASTM D7913/D7913M-14 standard test method for bond strength of fiber-reinforced polymer matrix composite bars to concrete by pullout testing*. 2014, ASTM International: West Conshohocken, PA.

41. Fergani, H., et al., *Durability and degradation mechanisms of GFRP reinforcement subjected to severe environments and sustained stress.* Construction and Building Materials, 2018. 170: p. 637-648.

42. Almusallam, T.H., et al., *Tensile properties degradation of glass fiber-reinforced polymer bars embedded in concrete under severe laboratory and field environmental conditions.* Journal of Composite Materials, 2013. 47(4): p. 393-407.

43. Park, Y., *Long-term performance of GFRP reinforced concrete beams and bars subjected to aggressive environments*. 2012, University of Texas at Arlington.

44. Bakis, C.E., et al., *Tensile strength of GFRP bars under sustained loading in concrete beams.* ACI Special Publication, 2005. 230: p. 1429-1446.

45. Davalos, J.F., Y. Chen, and I. Ray, *Effect of FRP bar degradation on interface bond with high strength concrete.* Cement and Concrete Composites, 2008. 30(8): p. 722-730.

46. Bazli, M., H. Ashrafi, and A.V. Oskouei, *Experiments and probabilistic models of bond strength between GFRP bar and different types of concrete under aggressive environments.* Construction and Building Materials, 2017. 148: p. 429-443.

47. Wang, Z., et al., *Long-term durability of basalt- and glass-fibre reinforced polymer (BFRP/GFRP) bars in seawater and sea sand concrete environment.* Construction and Building Materials, 2017. 139: p. 467-489.

48. Mukherjee, A. and S.J. Arwikar, *Performance of glass fiber-reinforced polymer reinforcing bars in tropical environments- part II: Microstructural tests.* ACI Structural Journal, 2005. 102(6): p. 816-822.

49. Ruiz Emparanza A, et al., *Bond evaluation of GFRP reinforcing bars embedded in concrete under aggressive environments*, in *9th International Conference on Fibre-Reinforced Polymer Composites in Civil Engineering*. 2018: Paris.

50. Mohammed, T.U., H. Hamada, and T. Yamaji, *Performance of seawater-mixed concrete in the tidal environment.* Cement and Concrete Research, 2004. 34(4): p. 593-601.

51. Etxeberria, M., J.M. Fernandez, and J. Limeira, *Secondary aggregates and seawater employment for sustainable concrete dyke blocks production: Case study.* Construction and Building Materials, 2016. 113: p. 586-595.

52. Wegian, F.M., *Effect of seawater for mixing and curing on structural concrete.* The IES Journal Part A: Civil & Structural Engineering, 2010. 3(4): p. 235-243.

53. Abrams, D., A. , *Tests of impure waters for mixing concrete.* Proceedings of the American Concrete Institute, 1924. 20(2).

54. Steinour, H.H., *Concrete mix water - How impure can it be?* Research and Development Laboratories of the Portland Cement Association, 1960. 2(3): p. 32-50.

55. Dempsey, J.G., *Coral and salt water as concrete materials.* Journal Proceedings of American Concrete Institute, 1951. 48(10).

56. Nishida, T., et al., *Some considerations for applicability of seawater as mixing water in concrete.* Journal of Materials in Civil Engineering, 2015. 27(7): p. B4014004.

57. Furuya, D., N. Otsuki, and T. Saito, *A study on the effects of seawater as mixing water on the hydration characteristics of blast-furnace slag cement*, in *34th Conference on our World in Concrete & Structures*. 2009, CI-Premier PTE LTD: Singapore.

58. Katano, K., et al., *Properties and application of concrete made with sea water and un-washed sea sand* in *Third International Conference on Sustainable Construction Materials and Technologies*. 2013: Kyoto, Japan.

59. Kaushik, S.K. and S. Islam, *Suitability of sea water for mixing structural concrete exposed to a marine environment.* Cement and Concrete Composites, 1995. 17(3): p. 177-185.

60. Griffin, D.F. and R.L. Henry, *The effect of salt in concrete on compressive strength, water vapor transmission, and corrosion of reinforcing steel*. 1964, U.S. Naval Civil Engineering Laboratory: Port Hueneme, California. p. 45.

61. Taylor, M.A. and A. Kuwairi, *Effects of ocean salts on the compressive strength of concrete.* Cement and Concrete Research, 1978. 8(4): p. 491-500.

62. Otsuki, N., et al., *Possibility of sea water as mixing water in concrete*, in *36th Conference on our World in Concrete & Structures*. 2011: Singapore.

63. Montanari, L., et al., *Hydration, pore solution, and porosity of cementitious pastes made with seawater.* ASCE Journal of Materials in Civil Engineering, 2018. Submitted.

64. Shi, Z., et al., *Combined effect of metakaolin and sea water on performance and microstructures of concrete.* Construction and Building Materials, 2015. 74: p. 57-64.

65. Li, Q., et al., *Effect of metakaolin addition and seawater mixing on the properties and hydration of concrete.* Applied Clay Science, 2015. 115: p. 51-60.

66. Jensen, H.U. and P.L. Pratt, *The effect of fly ash on the hydration of cements at low temperature mixed and cured in sea-water.* MRS Proceedings, 1987. 113: p. 279.

67. ASTM, *ASTM C143/C143M-15a standard test method for slump of hydraulic-cement concrete*. 2015, ASTM International: West Conshohocken, PA.

68. ASTM, *ASTM C138/C138M-17a standard test method for density (unit weight), yield, and air content (gravimetric) of concrete*. 2017, ASTM International: West Conshohocken, PA.

69. ASTM, *ASTM C231/C231M-17a standard test method for air content of freshly mixed concrete by the pressure method*. 2017, ASTM International: West Conshohocken, PA.

70. ASTM, *ASTM C191-18 standard test methods for time of setting of hydraulic cement by vicat needle*. 2018, ASTM International: West Conshohocken, PA.

71. ASTM, *ASTM C305-14 standard practice for mechanical mixing of hydraulic cement pastes and mortars of plastic consistency*. 2014, ASTM International: West Conshohocken, PA.

72. ASTM, *ASTM C39/C39M-18 standard test method for compressive strength of cylindrical concrete specimens*. 2018, ASTM International: West Conshohocken, PA.

73. weather.com. *Coral Gables, FL monthly weather*. 2018.

74. Goldston, J.S., *Influence of biscayne bay's salinity regime on gulf pipefish (syngnathus scovelli) trends of abundance and distribution*, in *Rosenstiel School of Marine and Atmospheric Science*. 2017, University of Miami.

75. Higginson, E., C. , *Effect of steam curing on the important properties of concrete.* Journal Proceedings of American Concrete Institute, 1961. 58(9): p. 281-298.

76. Khatibmasjedi, M., et al., *Durability of GFRP reinforcement in seawater-mixed concrete under accelerated aging conditions.* ASCE Journal of Composites for Construction, 2018. Submitted.

77. Hooton, R.D. and M.P. Titherington, *Chloride resistance of high-performance concretes subjected to accelerated curing.* Cement and Concrete Research, 2004. 34(9): p. 1561-1567.

78. Suraneni, P., et al., *Calcium Oxychloride formation potential in cementitious pastes exposed to blends of deicing salt.* ACI Materials Journal, 2017. 114(4): p. 631-641.

79. Spragg, R., *Development of performance related specifications that include formation factor*, in *School of Civil Engineering*. 2017, Purdue University: West Lafayette, Indiana. p. 205.

80. Weiss, W., et al., *Toward a specification for transport properties of concrete based on the formation factor of a sealed specimen.* Advances in Civil Engineering Materials, 2016. 5(1): p. 179-194.

81. Spragg, R., C. Villani, and J. Weiss, *Electrical properties of cementitious systems: Formation factor determination and the influence of conditioning procedures.* Advances in Civil Engineering Materials, 2016. 5: p. 124-148.

82. Spragg, R., et al., *Leaching of conductive species: Implications to measurements of electrical resistivity.* Cement and Concrete Composites, 2017. 79: p. 94-105.

83. Snyder, K.A., et al., *Estimating the electrical conductivity of cement paste pore solutions from OH^-, K^+ And Na^+ concentrations.* Cement and Concrete Research, 2003. 33(6): p. 793-798.

84. Rogers, C. and R. Hooton, *Reduction in mortar and concrete expansion with reactive aggregates due to alkali leaching.* Cement, Concrete and Aggregates, 1991. 13(1): p. 42-49.

85. Famy, C., et al., *Influence of the storage conditions on the dimensional changes of heat-cured mortars.* Cement and Concrete Research, 2001. 31(5): p. 795-803.

86. Islam, M.M., et al., *Suitability of sea water on curing and compressive strength of structural concrete.* Journal of Civil Engineering (IEB), 2012. 40(1): p. 37-45.

87. Qiao, C., P. Suraneni, and J. Weiss, *Damage in cement pastes exposed to NaCl solutions.* Construction and Building Materials, 2018. 171: p. 120-127.

88. Lim, E.D., et al., *Strength and corrosion behavior of mortar mixed and/or cured with seawater with various fly ash replacement ratios.* Asian Journal of Civil Engineering, 2015. 16(6): p. 835-849.

89. Polder, R.B., *Test methods for on site measurement of resistivity of concrete — a RILEM TC-154 technical recommendation.* Construction and Building Materials, 2001. 15(2): p. 125-131.

90. Radlinska, A., et al., *Shrinkage mitigation strategies in cementitious systems: A closer look at differences in sealed and unsealed behavior.* Transportation Research Record, 2008. 2070(1): p. 59-67.

91. Hajibabaee, A. and M.T. Ley, *Impact of wet and sealed curing on curling in cement paste beams from drying shrinkage.* ACI Materials Journal, 2015. 112(1).

92. Sant, G., P. Lura, and J. Weiss, *Measurement of volume change in cementitious materials at early ages: Review of testing protocols and interpretation of results.* Transportation Research Record: Journal of the Transportation Research Board, 2006. 1979: p. 21-29.

93. Li, H., N. Farzadnia, and C. Shi, *The role of seawater in interaction of slag and silica fume with cement in low water-to-binder ratio pastes at the early age of hydration.* Construction and Building Materials, 2018. 185: p. 508-518.

94. Suryavanshi, A.K., J.D. Scantlebury, and S.B. Lyon, *Pore size distribution of OPC & SRPC mortars in presence of chlorides.* Cement and Concrete Research, 1995. 25(5): p. 980-988.

95. Park, S.S., S.-J. Kwon, and H.-W. Song, *Analysis technique for restrained shrinkage of concrete containing chlorides.* Materials and Structures, 2011. 44(2): p. 475-486.

96. Mehta PK and P. Monteiro, *Concrete: Microstructure, properties, and materials*. 3rd ed. 2006, New York, NY: McGraw-Hill.

97. Khatibmasjedi, M., et al., *Compressive strength development of concrete mixed with seawater subject to different curing regimes.* ACI Materials Journal, 2018. Submitted.

98. ASTM, *ASTM C778-17 standard specification for standard sand*. 2017, ASTM International: West Conshohocken, PA.

99. ASTM, *ASTM C1698 - 09(2014) standard test method for autogenous strain of cement paste and mortar*. 2014, ASTM International: West Conshohocken, PA.

100. ASTM, *ASTM C596-09(2017) standard test method for drying shrinkage of mortar containing hydraulic cement*. 2017, ASTM International: West Conshohocken, PA.

101. Poursaee, A. and C.M. Hansson, *Reinforcing steel passivation in mortar and pore solution.* Cement and Concrete Research, 2007. 37(7): p. 1127-1133.

102. Lee, H.K., K.M. Lee, and B.G. Kim, *Autogenous shrinkage of high-performance concrete containing fly ash.* Magazine of Concrete Research, 2003. 55(6): p. 507-515.

103. Chindaprasirt, P., C. Jaturapitakkul, and T. Sinsiri, *Effect of fly ash fineness on compressive strength and pore size of blended cement paste.* Cement and Concrete Composites, 2005. 27(4): p. 425-428.

104. Khatibmasjedi, S., *Insights into the mechanisms of salt scaling of high volume fly ash concrete*. 2014, Oklahoma State University: Stillwater, OK.

105. Dhandapani, Y., et al., *Mechanical properties and durability performance of concretes with limestone calcined clay cement (LC^3).* Cement and Concrete Research, 2018. 107: p. 136-151.